Load flow and state estimation algorithms for three-phase unbalanced power distribution systems

By

Chiranjeevi Madvesh

A Thesis
Submitted to the Faculty of
Mississippi State University
in Partial Fulfillment of the Requirements
for the Degree of Master of Science
in Electrical Engineering
in the Department of Electrical and Computer Science Engineering

Mississippi State, Mississippi

August 2014

Load flow and state estimation algorithms for three-phase unbalanced power distribution systems

By

Chiranjeevi Madvesh

Approved:

_____

Yong Fu
(Major Professor)

_____

Stanislaw Grzybowski
(Committee Member)

_____

Sherif Abdelwahed
(Committee Member)

_____

James E. Fowler
(Graduate Coordinator)

_____

Jason M. Keith
Dean
Bagley College of Engineering

Name: Chiranjeevi Madvesh

Date of Degree: August 15, 2014

Institution: Mississippi State University

Major Field: Electrical Engineering

Major Professor: Yong Fu

Title of Study: Load flow and state estimation algorithms for three-phase unbalanced power distribution systems

Pages in Study: 99

Candidate for Degree of Master of Science

Distribution load flow and state estimation are two important functions in distribution energy management systems (DEMS) and advanced distribution automation (ADA) systems. Distribution load flow analysis is a tool which helps to analyze the status of a power distribution system under steady-state operating conditions. In this research, an effective and comprehensive load flow algorithm is developed to extensively incorporate the distribution system components. Distribution system state estimation is a mathematical procedure which aims to estimate the operating states of a power distribution system by utilizing the information collected from available measurement devices in real-time. An efficient and computationally effective state estimation algorithm adapting the weighted-least-squares (WLS) method has been developed in this research. Both the developed algorithms are tested on different IEEE test-feeders and the results obtained are justified.

DEDICATION

I would like to dedicate this research to my parents, brother, sisters and friends.

ACKNOWLEDGEMENTS

I would like to express my gratitude to my major advisor, Dr. Yong Fu for his constant support, guidance and encouragement during the course of this research. This work would not have been possible without his guidance. He has not only guided my thesis work but also enlightened my personality and professional attitude at personal level. He gave me opportunities to work on multiple projects which enhanced my knowledge and gave me recognition.

I am very grateful to Dr. Stanislaw Grzybowski and Dr. Sherif Abdelwahed for their support, valuable comments and willingness to serve on my graduate committee.

I wish to thank my parents for their blessings and motivation which helped me to pursue my Master's degree. The constant support and encouragement from my brother, sisters and friends helped me to boost my confidence and achieve success.

TABLE OF CONTENTS

DEDICATION ii

ACKNOWLEDGEMENTS iii

LIST OF TABLES vii

LIST OF FIGURES ix

CHAPTER

I. INTRODUCTION 1

1.1 Introduction 1
1.2 Types of distribution system 2
1.2.1 Simple Radial Networks 3
1.2.2 Simple Loop Networks 4
1.2.3 Hybrid Radial-Loop Networks 5
1.2.4 Simple Spot Networks 6
1.2.5 Medium Voltage AC, AC/DC Networks 7
1.3 Background for load flow and state estimation 8
1.4 Research objective and contribution 10
1.5 Thesis Overview 12

II. A COMPREHENSIVE LOAD FLOW ALGORITHM FOR A THREE PHASE UNBALANCED RADIAL POWER DISTRIBUTION NETWORK 13

2.1 Introduction 13
2.2 Three phase line models 14
2.3 Carson's equation and Kron's reduction 16
2.3.1 Carson's equation 16
2.3.2 Kron's Reduction 17
2.4 Types of loads 18
2.4.1 Wye connected loads 19
2.4.1.1 Constant impedance loads (CZ) 20
2.4.1.2 Constant current loads (I) 20
2.4.1.3 Constant Power Loads (P) 21
2.4.2 Delta Connected Loads 21
2.4.2.1 Constant Impedance Loads (Z) 21
2.4.2.2 Constant Current Loads (I) 22
2.4.2.3 Constant Power Loads (P) 22
2.5 Types of three phase transformers 23
2.5.1 Transformation matrices and Thevenin equivalent circuit 24
2.5.1.1 Voltage transformation matrices 24

2.5.1.2 Current transformation matrices 26
2.5.1.3 Thevenin equivalent circuit....27
2.5.2 Delta – Grounded wye connection....29
2.5.3 Delta – Delta connection....31
2.5.4 Grounded Wye – Grounded Wye connection....32
2.5.5 Grounded wye – Delta connection....33
2.6 Voltage regulators....35
2.6.1 Wye connected three-phase voltage regulators....35
2.6.2 Delta connected three-phase voltage regulator....37
2.7 Shunt capacitors....39
2.7.1 Wye connected shunt capacitors....39
2.7.2 Delta connected shunt capacitors....40
2.8 Switches....41
2.9 Load flow algorithm....42
2.9.1 Development of bus-injection to branch-current (BIBC) matrix....43
2.9.1.1 Algorithm development....43
2.9.1.2 BIBC formation procedure for an n-bus distribution system....45
2.9.2 Development of branch-current to bus-voltage (BCBV) matrix....46
2.9.2.1 Algorithm development....46
2.9.2.2 BCBV formation procedure for an n-bus distribution system....47
2.9.3 Adjustment matrix....48
2.9.3.1 Improvisation of BCBV matrix....49
2.9.3.2 Improvisation of BIBC matrix....51
2.9.4 Load flow Solution Technique....53

III. STATIC STATE ESTIMATION FOR A THREE-PHASE UNBALANCED RADIAL POWER DISTRIBUTION NETWORKS....54

3.1 Introduction....54
3.2 State estimation procedure....56
3.3 Weighted least square method....57
3.4 State estimation formulation for a three phase power distribution network....60
3.4.1 Measurement Data....61
3.4.2 Mathematical model....62
3.4.3 Observability Analysis based Measurement Selection Technique (OA-MST)....62
3.4.4 Load Modeling Technique (LMT) for distribution system state estimation....63
3.4.5 Algorithm development....65

IV. RESULTS AND DISCUSSION....67

4.1 Load flow results....67
4.1.1 IEEE – 4 bus system....67
4.1.2 IEEE – 13 bus system....71
4.1.3 IEEE – 37 bus system....73
4.2 State estimation results....76
4.2.1 IEEE – 4 bus system....77
4.2.2 IEEE – 13 bus system....81
4.2.3 IEEE – 37 bus system....83

V. CONCLUSION AND FUTURE WORK....85

5.1 Conclusion....85
5.2 Future work....86

REFERENCES....87

APPENDIX

A. JACOBIAN MATRIX FOR STATE ESTIMATION OF A THREE PHASE DISTRIBUTION NETWORK....90

A.1 The elements of Jacobian matrix are expressed as,....91

B. DISTRIBUTION SYSTEM PARAMETERS....93

B.1 IEEE – 4 bus system....94
B.2 IEEE – 13 bus system....95
B.3 IEEE – 37 bus system....97

LIST OF TABLES

4.1 Three phase load data of IEEE – 4 bus feeder 68

4.2 Three phase Transformer data of IEEE – 4 bus feeder 68

4.3 Capacitor Data of IEEE – 4 bus system 68

4.4 Regulator Data of IEEE – 4 bus feeder 68

4.5 Load flow results for an IEEE 4– bus with different types of transformers 70

4.6 Comprehensive load flow results for an IEEE 4– bus feeder 71

4.7 Comprehensive load flow results for an IEEE 13– bus feeder 73

4.8 Comprehensive load flow results for an IEEE 37– bus feeder 75

4.9 Observations 76

4.10 Voltage Measurement Data for 4 – bus feeder 78

4.11 Power Flow Measurement Data for 4 – bus feeder 78

4.12 Injected Power Measurement Data for 4 – bus feeder 78

4.13 Current Flow Measurement Data for 4 – bus feeder 78

4.14 Selection Criteria Vector 80

4.15 State Variables obtained for a 4 – bus feeder 80

4.16 Observations 81

4.17 State Variables obtained for a 13 – bus feeder with only CP loads 81

4.18 State Variables obtained for a 13 – bus feeder with only CP, CZ & CI loads 83

4.19 State Variables obtained for a 37-bus test feeder 84

B.1 Data for three phase transformer....94
B.2 Load data....94
B.3 Network topology data....95
B.4 Data for three phase transformer....95
B.5 Shunt capacitor data....95
B.6 Three phase voltage regulator data....95
B.7 Load data for spot loads....96
B.8 Load data for distributed loads....96
B.9 Data for three phase transformer....97
B.10 Load data for spot loads....97
B.11 Network topology data....98
B.12 Three phase voltage regulator data....99

LIST OF FIGURES

1.1 Typical power system components 2

1.2 IEEE 13 bus radial type test feeder 4

1.3 Simple Loop Network 5

1.4 Hybrid Radial-Loop Network 6

1.5 Simple Spot Network 7

1.6 MVDC ship power system model [3] 8

2.1 Three-phase four wire line model 15

2.2 Three - phase wye connected load 19

2.3 Three-phase delta connected load 21

2.4 Three bus system 27

2.5 Delta – Grounded Wye Transformer 29

2.6 Delta – Delta transformer 31

2.7 Grounded Wye – Grounded Wye transformer 32

2.8 Grounded wye – Delta transformer 34

2.9 Three phase wye connected voltage regulator 36

2.10 Three phase delta connected voltage regulator 38

2.11 Wye – connected capacitor bank 39

2.12 Delta connected capacitor bank 40

2.13 Modified IEEE-4 bus test feeder 44

2.14 Flow chart for BIBC matrix formation 47

2.15 Flow chart for BCBV matrix formation.....48

2.16 Comprehensive IEEE 4- bus Network – modified 49

3.1 Three-phase measurement unit symbols.....61

3.2 Flow chart for observability analysis.....64

4.1 IEEE - 4 bus test system 67

4.2 IEEE - 13 bus test system 72

4.3 IEEE -37 bus test system 74

4.4 Modified IEEE 4-bus system with measurement units.....77

4.5 Modified IEEE-13 bus test system with measurement units 82

CHAPTER I

INTRODUCTION

1.1 Introduction

Three phase power distribution networks are one of the most complicated grid interconnection in the entire electric power systems. Since the invention of electricity and its distribution to consumers, there has been a lot of improvement at the generating stations, transmission lines, insulators, protection devices, components of power system etc., but the distribution system remained to be same with no major changes or improvement.

Today's modern world has taken the electrical energy for granted and it has become a part of basic necessity. As the future is progressing at a fast pace towards making the electric grids much smarter, autonomous, reliable and having enhanced ability to incorporate many number of distributed generations, resulting in smart micro-grids, it is of utmost important for the power distribution networks to operate at its full efficiency with high reliability and hence is the necessity for power distribution network analysis.

As seen in the Figure 1.1, the power distribution networks come into play only from the substations and extend itself till the consumer end where it is metered and billed. Most of the distribution feeders originate at substation, and they in-turn serve one or more secondary feeders.

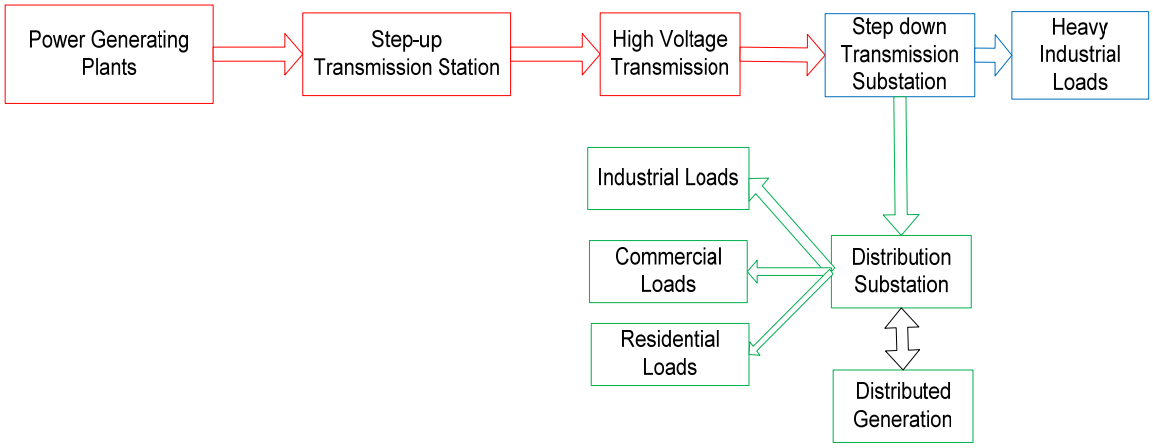

Figure 1.1 Typical power system components

In this case, it has become obvious that the distribution system is radial in nature, which implies that the power flow is only in one direction i.e. from substations to the consumer's loads. Based on the requirements, the distribution network can be modeled into various types which are explained in the following section.

1.2 Types of distribution system

Distribution system often works at voltages levels around 13.2 kV, 4.16 kV etc. which is later reduced to customer utilization voltage level i.e. around 120 volts phase-neutral using a transformer. The primary voltage levels at the distribution substations in the United States ranges from 2.4 kV to 69 kV, which are fed by the high voltage transmission or sub transmission lines. 11kV and 33 kV distribution voltage levels are very common in the European and Middle Eastern countries with the customer utilization voltage level around 230 volts phase-neutral [1].

In this study, the radial type distribution network is preferred because of its vast usage in the current scenario of three phase distribution systems. In certain cases,

different types of distribution system is applicable where the customer is a small scale industry or a commercial building, where the voltage and power required are comparatively higher than that of domestic loads [1] and [2].

This section explains about the major types of distribution networks available today, they are:

- Simple Radial Network
- Simple Loop Network
- Hybrid Radial-Loop Networks
- Simple Spot Networks and
- Medium Voltage AC, AC/DC Network

1.2.1 Simple Radial Networks

Radial Distribution Networks are most commonly used due to their simplicity in design, analysis, low maintenance and cost effectiveness. Simple radial type distribution feeders are modeled by a single or one way path for the power to flow i.e. from the substation (source) to the customers (loads). A conventional radial distribution network consists of one or more substations and multiple feeders with network components like voltage regulators, shunt capacitance, distribution transformers etc. to deliver the power at customer voltage levels.

Analysis of this type of network is comparatively easier than other types available. As the load is served from a single substation in most cases, full advantage can be taken among the diversity of loads but at the cost of poor voltage regulation and

efficiency for the customers at the end of feeders. This issue can be resolved using the network components like step-up voltage regulators and shunt capacitors.

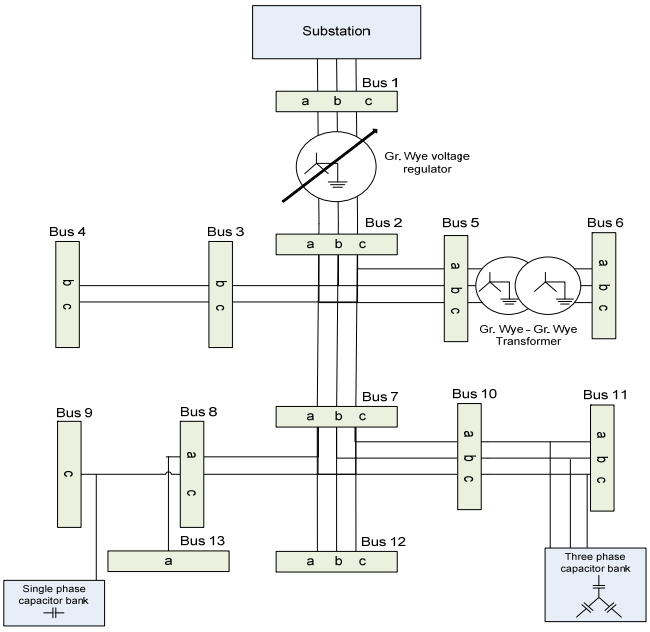

Figure 1.2 IEEE 13 bus radial type test feeder

In this research, we have considered radial distribution feeders for our load flow analysis and state estimation. Figure 1.2 shows the structure of a simple radial distribution network.

1.2.2 Simple Loop Networks

Loop type distribution feeders are characterized by having two or more paths for power transfer from substation (source) to customers (loads). This type of networks can supply the power to customers from either path as shown in Figure 1.3. The loop type

distribution feeders are often designed to work as radial type by strategic placements of circuit breakers/switches.

The loop type is more reliable compared to radial type feeders, but it is not economical due to the requirement of more number of circuit breakers, conductors and automation equipment's [1] and [2].

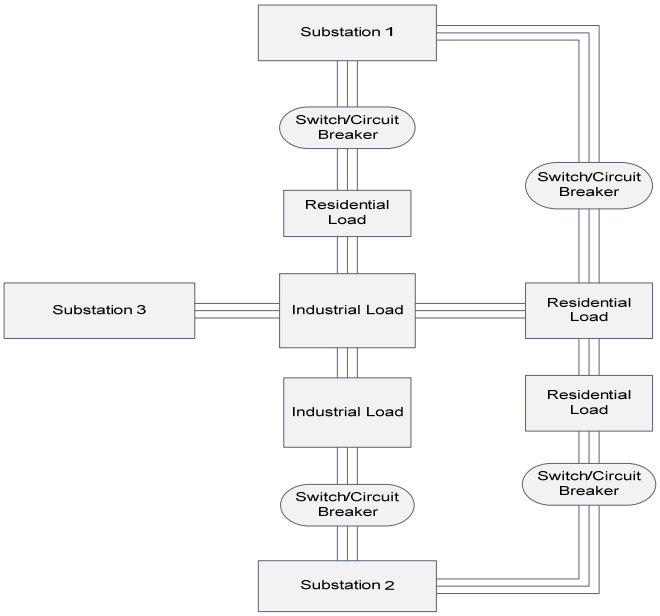

Figure 1.3 Simple Loop Network

1.2.3 Hybrid Radial-Loop Networks

As the name itself suggest, this type of networks consists of a combination of radial and loop type feeder design.

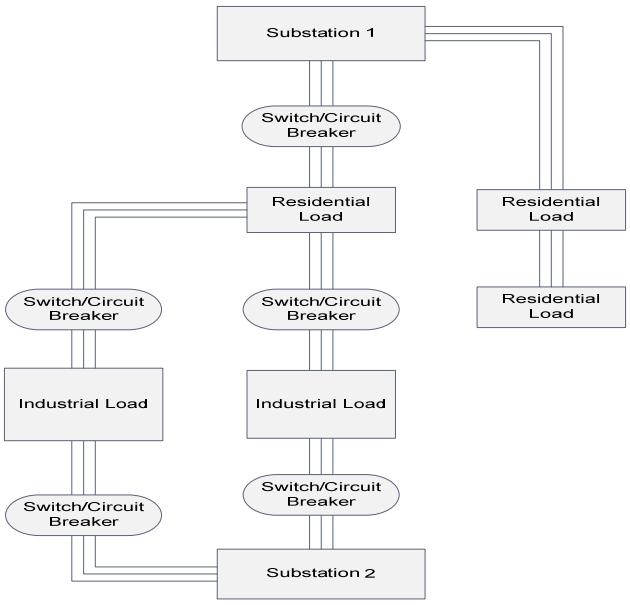

Figure 1.4 Hybrid Radial-Loop Network

They mainly consist of one or more loops at the substation end and radial-type at the customer end or vice-versa as shown in the Figure 1.4. These types of networks are highly reliable and mostly used at high density areas and city downtowns where reliability is of utmost importance [1] and [2].

1.2.4 Simple Spot Networks

Simple spot networks are similar to radial type network but on a smaller scale. These types of networks are implemented near huge buildings or sky-scrapers which have multiple loads with high power consumption at customer voltage levels. They are reliable and economical for power delivery covering small areas and short distances [1] and [2]. A model of simple spot network is shown below.

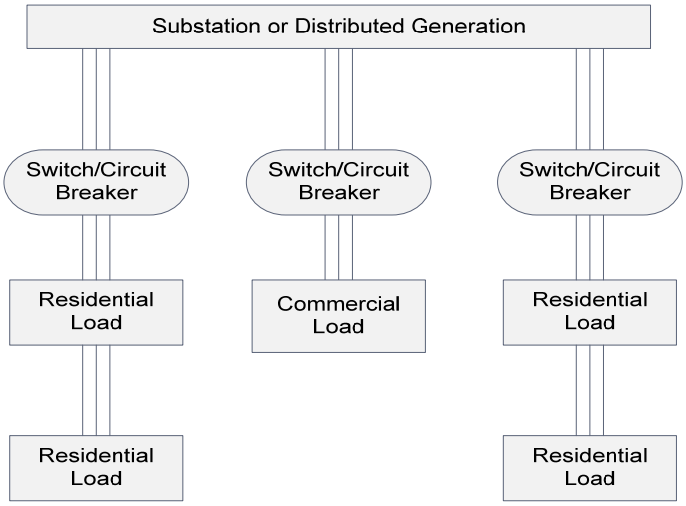

Figure 1.5 Simple Spot Network

1.2.5 Medium Voltage AC, AC/DC Networks

Now-a-days, medium voltage AC/DC networks are gaining high popularity. These types of networks are mostly used when the grid or utility is not available. The source is mostly a turbine-generator or renewable energy source with a single bus. All the feeders are connected to the same bus in the form of a ring. This system can incorporate multiple generators when a single generator does not have the adequate capacity to feed the load.

The design and analysis of medium voltage AC/DC networks are comparatively very complicate due to the presence of high power rating power electronic converters. Considerable research is being done to introduce this type of network for shipboard power systems [3]. The diagram of a MVDC ship power system is as shown below.

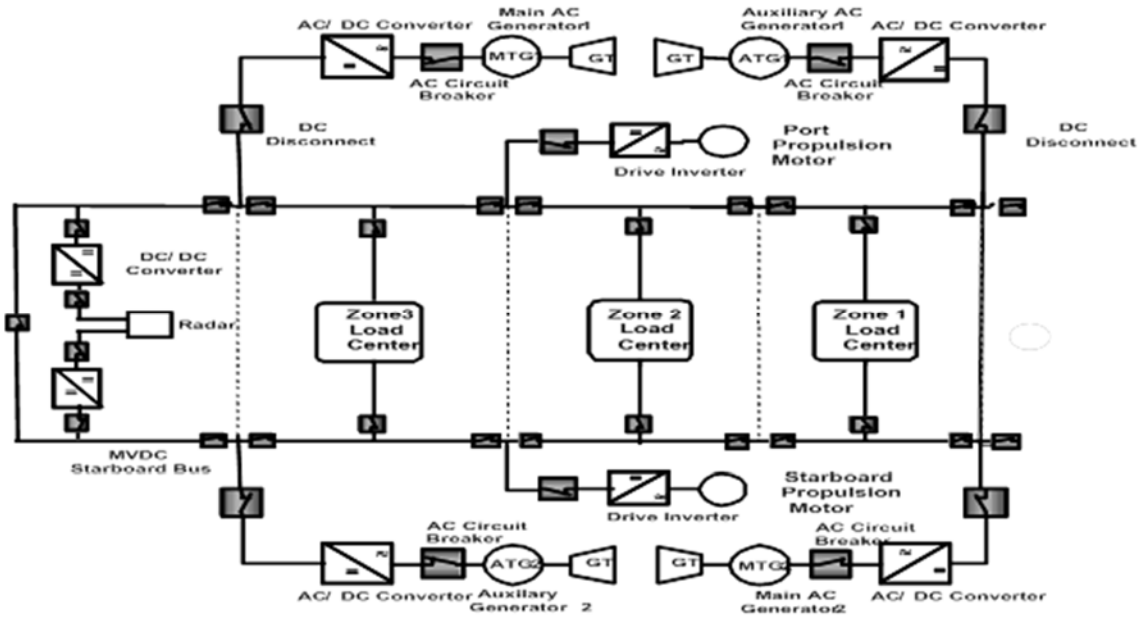

Figure 1.6 MVDC ship power system model [3]

1.3 Background for load flow and state estimation

In recent years, extensive research has been done in the area of load flow studies for a three phase distribution system. Due to its high resistance by reactance ratio (R/X), unbalanced loads, multi-phase and un-transposed lines, the regular procedures such as the Newton-Raphson, Gauss-Seidal and Decouple / Fast Decoupled load flow methods might not converge and may provide inaccurate load-flow results [4] and [5].

In order to design an accurate load flow tool considering all the distribution system characteristics as mentioned above, several authors have proposed different methods and approaches as given in publications [6] - [8].

Few of the highly accepted methods for distribution load flow analysis are Gauss-implicit method in [9], forward/backward sweep algorithm in [10], a modified Newton method for radial distribution system load flow is discussed in [11], a current injection

based load flow method has been developed in [12], however, most of these developed algorithms have not considered the effects of distribution system components like shunt capacitor, load models, three phase transformers, voltage regulators or circuit breaker status in their load flow algorithm, hence they are not comprehensive in nature.

Usually, all the electric power systems operates in three different states, they are, normal or secure state, emergency state and restorative state [13]. These operating states can be determined by knowing the topology of the network, voltage magnitude and phase angles at every bus.

The real-time data from measurements units located at various locations are used to monitor the power system operating state. But, we must understand that the raw data from measurement devices might not be accurate all the time and sometimes the data available might be insufficient to determine the operating state. Hence, in order to overcome this problem, all the available measurement data must be processed by using a technique known as State Estimation [13].

Power system state estimator (PSSE) forms the base for energy management systems (EMS), distribution management system (DMS) and real-time/online security analysis. They are capable of filtering out the redundant data received from the measuring devices which is very crucial in determining the state variables very precisely. This precision is necessary for a power system which in turn helps to study security assessment, load shedding, blackout prevention, contingency analysis and optimal load flow etc. State estimators are most useful for efficient and accurate monitoring of these operational states.

Various methods have been developed on state estimation procedure for power distribution networks. One of the first research papers on distribution system state estimation was published in the year 1995 by C.N. Lu et al. [14] which was on current based state estimation. In this paper, the author provided a lot of scope for future researchers to focus on distribution system state estimation. In [15] state estimation formulations for specific three phase models were carried out. For the first time, a state estimation model for three phase power system adapting the traditional weighted least square (WLS) method is discussed in [16]. Few highly appreciated works related to three-phase distribution system state estimation is explained in [17] and [18]. A state estimation procedure using the traditional forward-backward sweep method was developed in [19]. Preliminary work on 'state estimation and impacts of load modeling' is published in [20].

1.4 Research objective and contribution

There are two main objectives in this research, they are:

1) To develop an effective and comprehensive load flow algorithm for a three phase unbalanced radial type power distribution network.
2) To develop an efficient and computationally effective state estimation tool for a three phase unbalanced power distribution system.

Therefore, to accomplish the first objective,

- A generalized load flow algorithm is developed in which all the network parameters and components are modeled extensively to suit the load flow algorithm.
- The existing load flow algorithm has been extended by addition of three different matrices which are developed in this research. These matrices are

voltage adjustment matrix, current adjustment matrix and impedance adjustment matrix. These three developed matrices play a key role in incorporating all the distribution system components which includes three-phase line models, radial structure, three phase loads, three different types of load models, shunt capacitors, three-phase voltage regulators, four types of three-phase transformers, and switches/circuit breakers.

When all the above mentioned distribution system components and parameters are incorporated in the load flow algorithm, the results such as voltage magnitude and phase angles obtained at each bus are more accurate.

In order to achieve the second objective,

- The power flow equations are modeled for a three phase distribution system and state estimation (SE) algorithm is solved using the weighted least square (WLS) method.
- Two new concepts are introduced in this part of research. One of them is load modelling technique **(**LMT) and the other is observability analysis based measurement selection technique (OA-MST). The LMT helps in improving the accuracy of the state variables calculated by the algorithm and the OA-MST will help to reduce the computational time of the SE algorithm.

These obtained state variables in real-time will allow the system operator to ascertain the operating state of a power distribution network.

1.5 Thesis Overview

The thesis is organized as follows,

Chapter II explains about the modeling of distribution system components such as three phase line models, three-phase transformers, load types, shunt capacitors, voltage regulators and switches. It also reviews the existing load flow models and a detailed description of the developed load flow algorithm is given.

Chapter III discusses the state estimation procedure for radial three phase distribution networks. It presents the equations modeled and highlights the developed state estimation algorithm with observability analysis and load modeling.

Chapter IV contains the results of the developed algorithm for three case studies i.e. IEEE – 4 bus, IEEE – 13 bus and IEEE – 37 bus test feeders. The results obtained are discussed and summarized for both load-flow and state estimation algorithms.

Chapters V, gives a brief summary about the current research work and mentions the possible ideas for the future which can be done in the area of power distribution system automation.

CHAPTER II

A COMPREHENSIVE LOAD FLOW ALGORITHM FOR A THREE PHASE UNBALANCED RADIAL POWER DISTRIBUTION NETWORK

2.1 Introduction

For any given power system, load flow analysis is an important and basic task. Many applications like distribution automation, state estimation, contingency analysis, optimal load flow, network optimization etc. are dependent on the load flow solution. Hence a comprehensive load flow tool specifically designed for three phased unbalanced radial distribution network is required [5] and [21].

Most of the power distribution systems today are either radial or hybrid radial-loop in nature [6], which requires an iterative scheme for solving load-flow problems. The existing load-flow algorithms which are used for transmission system analysis cannot be used directly used on distribution system analysis due to their poor convergence property [7] and [8]. Therefore, a new method, specially designed for radial, multi-phase distribution network is developed.

This chapter presents a comprehensive load flow algorithm for a three phase unbalanced radial power distribution network. The proposed method involves calculation of simple algebraic equations which are formulated using the network topology of the distribution system. The complex phasor voltage and current values for a three phase power system considering all the distribution system components (viz. three phase

transformers, voltage regulators, shunt capacitors and switches) are determined using the proposed algorithm. This method is also capable of incorporating distributed generations /renewable energy resources as well. This developed load flow method can be directly applied to any of the existing three phase power distribution systems.

The fundamental ideology for this research can be credited to the network topology method by A. Alsaadi and B. Gholami [4]. They have proposed two matrices viz. 'bus-injection to branch-current' (BIBC) and 'branch-current to bus-voltage' (BCBV) matrices which are constructed based on the network topology. These two matrices are used to determine the load flow solution. But their research did not include the effects of distribution system components like three phase transformers, shunt capacitor, switch status, voltage regulators and specific load models. Whereas, in this research we have included the effects of all the above mentioned distribution system components in our developed load flow algorithm.

Modeling of the network parameters and distribution components are explained in next sections. These are required prior to implementing load flow algorithm.

2.2 Three phase line models

The most common configuration of three phase lines in radial type distribution system consists of either overhead lines or underground cables [2]. Since the distribution system consists of multi-phase lines (i.e. three phase, two phase or single phase) serving loads which are mostly unbalanced in nature, it is necessary to consider the self-impedance and mutual impedance of a given line. Self-impedance of a distribution line can be defined as the series impedance of a transposed line between two buses and the impedance value between two different phase conductors is known as mutual impedance.

General representation of a three phase feeder with self-impedance and mutual impedance of a line 'Aa' is shown in Figure 2.1, where Z_{aa}, Z_{bb}, Z_{cc} and Z_{nn} are self impedance of phase A, B, C and neutral respectively and $Z_{ab}, Z_{bc}, Z_{ca}, Z_{na}, Z_{nb}$ and Z_{nc} are mutual impedance between phase-to-phase and phase-to-neutral respectively.

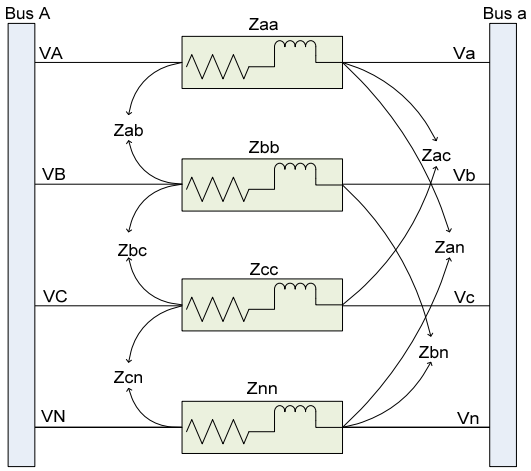

Figure 2.1 Three-phase four wire line model

The basic model consists of a three phase four wire system; this model is later transformed in to three phase three wire system based on Kron's reduction technique for computational efficiency [22]. The impedance matrix is given below (2.1) and (2.2).

$$[Z_{abcn}] = \begin{bmatrix} Z_{aa} & Z_{ab} & Z_{ac} & Z_{an} \\ Z_{ba} & Z_{bb} & Z_{bc} & Z_{bn} \\ Z_{ca} & Z_{cb} & Z_{cc} & Z_{cn} \\ Z_{na} & Z_{nb} & Z_{nc} & Z_{nn} \end{bmatrix} \frac{\Omega}{mile} \tag{2.1}$$

After Kron's reduction,

$$[Z_{abc}] = \begin{bmatrix} Z_{aa-n} & Z_{ab-n} & Z_{ac-n} \\ Z_{ba-n} & Z_{bb-n} & Z_{bc-n} \\ Z_{ca-n} & Z_{cb-n} & Z_{cc-n} \end{bmatrix} \frac{\Omega}{mile} \tag{2.2}$$

In a distribution system, there are many two phase and single phase connections along with three phase connections, between any two different nodes/buses. In this case the corresponding row and column of the impedance matrix are replaced with zeroes. It is as shown in (2.3) where phase b is absent and in (2.4) where phases a and c are absent,

$$[Z_{ac}] = \begin{bmatrix} Z_{aa} & 0 & Z_{ac} \\ 0 & 0 & 0 \\ Z_{ca} & 0 & Z_{cc} \end{bmatrix} \frac{\Omega}{mile} \tag{2.3}$$

$$[Z_b] = \begin{bmatrix} 0 & 0 & 0 \\ 0 & Z_{bb} & 0 \\ 0 & 0 & 0 \end{bmatrix} \frac{\Omega}{mile} \tag{2.4}$$

2.3 Carson's equation and Kron's reduction

This section explains in brief about the importance of modified Carson's equations and Kron's reduction technique in the analysis of power distribution system.

2.3.1 Carson's equation

During the initial stages of distribution system design, it was observed that the effects of phase impedance had to be considered for analysis because, the three phase conductors were not transposed and the loads were unbalanced on multi-phase systems. These are contradictory to the transmission line design. Therefore, for accurate analysis for a distribution system, major assumption of considering distribution system similar to transmission system cannot be made [22].

John Carson, in the year 1926, developed few equations which can determine the self-impedance and mutual impedance of a three-phase four line model by considering the effect of ground [22].

Due to computational complexity at that time, it was not of much importance. But later, with the evolution of computer technology and advance research has been done to modify the equation, and today it has become more feasible to use modified Carson's equations. These equations are simple and straight forward in terms of application. The modified Carson's equations are given as,

$$Z_{ii} = r_i + 0.09530 + j0.1234\left(ln\frac{1}{GMR_i} + 7.93\right)\Omega/mile \quad (2.5)$$

$$Z_{ij} = 0.09530 + j0.1234\left(ln\frac{1}{D_{ij}} + 7.93402\right)\Omega/mile \quad (2.6)$$

Where,

Z_{ii} is the line impedance

Z_{ij} is the phase impedance

r_i is the resistance of the distribution line

GMR_i is the geometric mean radius of distribution feeder

D_{ij} is the spacing between two conductors

2.3.2 Kron's Reduction

Kron's reduction technique was put forth in order to reduce the computation complexity and for a convenient representation of a three phase networks. Let us consider a three phase four-wire distribution system as shown in Figure 2.1 with a grounded neutral. The impedance matrix for this system is shown in Equation 2.1, which is a 4x4 matrix with the effect of neutral considered.

Since the neural is grounded, the voltage at bus 'A' and bus 'a' are equal. So, the initial 4x4 impedance matrix can be reduced to phase impedance 3x3 matrix as shown in

(2.7)-(2.9). This reduction holds good as long as Carson's equations are applied to find out self-impedance and mutual impedances, as they are calculated between each conductor and ground.

$$Z_{Premitive} = \begin{bmatrix} Z_{ij} & Z_{in} \\ Z_{nj} & Z_{nn} \end{bmatrix} \tag{2.7}$$

The 3x3 phase impedance matrix is obtained as,

$$Z_{abc} = [Z_{ij}] - [Z_{in}][Z_{nn}]^{-1}[Z_{nj}] \tag{2.8}$$

$$\therefore [Z_{abc}] = \begin{bmatrix} Z_{aa-n} & Z_{ab-n} & Z_{ac-n} \\ Z_{ba-n} & Z_{bb-n} & Z_{bc-n} \\ Z_{ca-n} & Z_{cb-n} & Z_{cc-n} \end{bmatrix} \frac{\Omega}{mile} \tag{2.9}$$

Where,

Z_{ij} is the phase impedance matrix of bus 'Aa'.

Z_{in} and Z_{nj} is the phase impedance matrix of bus 'Aa' with reference to neutral.

Z_{nn} is the neutral line impedance value of bus 'Aa'.

In most cases, the phase impedance matrix will be pre-determined during the design of a distribution system. This data can be directly used during analysis of the distribution networks. If the data is unavailable, then it is required to use both Carson's equations and Kron's reduction technique to calculate the 3x3 impedance matrix.

The above section explained about the modelling of three-phase line in a power distribution system. The next section discusses about the types of load.

2.4 Types of loads

Generally, two types of loads are considered in distribution network which are specified by their complex power consumption. They are spot loads which are connected

at the nodes and distributed loads which are connect along the length of the line. In most cases, the power demand will be specified as kW with power factor, kVA with power factor or kW and kVAr.

The loads on three phase distribution feeder can be classified in to four major groups, they are

- Constant Impedance (Z)
- Constant Current (I)
- Constant Power (P)
- Combination of ZIP or ZI or ZP or IP

The loads are further classified as three-phase wye connected loads and three phase delta connected loads. All the two-phase loads are connected between line to line and all single phase loads are connected between line and neutral and these loads can have any degree of unbalanced nature [9] and [23].

2.4.1 Wye connected loads

Wye connected load model is as shown below.

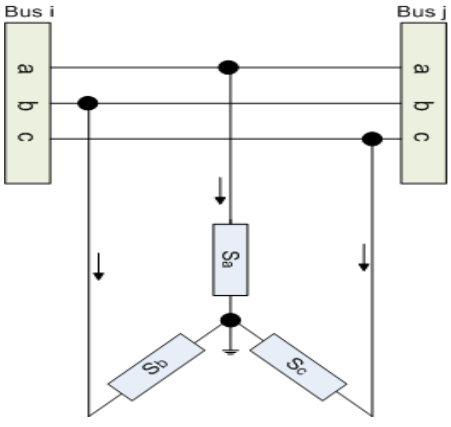

Figure 2.2 Three - phase wye connected load

2.4.1.1 Constant impedance loads (CZ)

From the prior known complex power and phase voltage value, we calculate the load impedance as shown below.

$$\begin{bmatrix} Z_a \\ Z_b \\ Z_c \end{bmatrix} = \begin{bmatrix} \frac{|V_{an}|^2}{S_a{}^*} \\ \frac{|V_{bn}|^2}{S_b{}^*} \\ \frac{|V_{cn}|^2}{S_c{}^*} \end{bmatrix} \tag{2.10}$$

The load impedance obtained is kept constant and does not change during iterations.

The load currents, which are now a function of constant load impedance, are calculated as shown in Equation 2.10. Here, the line-to-neutral complex voltage changes for every iteration.

$$\begin{bmatrix} I_a \\ I_b \\ I_c \end{bmatrix} = \begin{bmatrix} \frac{V_{an}}{Z_a} \\ \frac{V_{bn}}{Z_b} \\ \frac{V_{cn}}{Z_c} \end{bmatrix} \tag{2.11}$$

2.4.1.2 Constant current loads (I)

Here, the magnitude of the load current is calculated according to (2.12).

$$\begin{bmatrix} I_a \\ I_b \\ I_c \end{bmatrix} = \begin{bmatrix} \frac{S_a}{V_{an}} \\ \frac{S_b}{V_{bn}} \\ \frac{S_c}{V_{cn}} \end{bmatrix}^* \tag{2.12}$$

Now, the load current magnitudes obtained are held constant and the voltage angle (δ) changes on each iteration.

$$\begin{bmatrix} I_a \\ I_b \\ I_c \end{bmatrix} = \begin{bmatrix} |I_a| \angle \delta_a - \theta_a \\ |I_b| \angle \delta_b - \theta_b \\ |I_c| \angle \delta_c - \theta_c \end{bmatrix} \tag{2.13}$$

2.4.1.3 Constant Power Loads (P)

The load currents are calculated similar to Equation 2.12. Here the complex line-to-neutral voltage changes for every iteration till convergence is achieved.

2.4.2 Delta Connected Loads

Delta connected load model is shown in Figure 2.3. The equations used are much similar to start connected loads except for the complex power and the phasor voltages are phase-to-phase values.

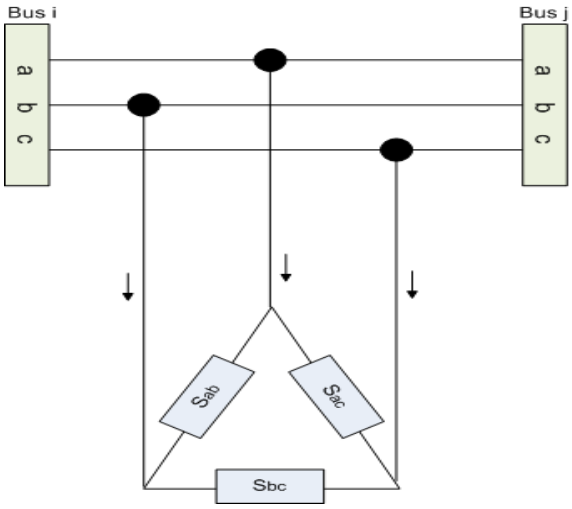

Figure 2.3 Three-phase delta connected load

2.4.2.1 Constant Impedance Loads (Z)

From the complex power specified and line voltages, the load impedance is determined as follows,

$$\begin{bmatrix} Z_{ab} \\ Z_{bc} \\ Z_{ca} \end{bmatrix} = \begin{bmatrix} \frac{|V_{ab}|^2}{S_{ab}{}^*} \\ \frac{|V_{bc}|^2}{S_{bc}{}^*} \\ \frac{|V_{ca}|^2}{S_{ca}{}^*} \end{bmatrix} \tag{2.14}$$

The load impedance is kept constant, only the phase-to-phase complex voltage will change during iterations.

$$\begin{bmatrix} I_{ab} \\ I_{bc} \\ I_{ca} \end{bmatrix} = \begin{bmatrix} \frac{V_{ab}}{Z_{ab}} \\ \frac{V_{bc}}{Z_{bc}} \\ \frac{V_{ca}}{Z_{ca}} \end{bmatrix} \tag{2.15}$$

2.4.2.2 Constant Current Loads (I)

The magnitude of the load current is calculated according to Equation 2.16.

$$\begin{bmatrix} I_{ab} \\ I_{bc} \\ I_{ca} \end{bmatrix} = \begin{bmatrix} \frac{S_{ab}}{V_{ab}} \\ \frac{S_{bc}}{V_{bc}} \\ \frac{S_{ca}}{V_{ca}} \end{bmatrix}^* \tag{2.16}$$

Now, the phase-to-phase load current magnitudes obtained are held constant, with the voltage angle (δ) varying at each iteration.

$$\begin{bmatrix} I_{ab} \\ I_{bc} \\ I_{ca} \end{bmatrix} = \begin{bmatrix} |I_{ab}|\angle\delta_{ab} - \theta_{ac} \\ |I_{bc}|\angle\delta_{bc} - \theta_{bc} \\ |I_{ca}|\angle\delta_{ca} - \theta_{ca} \end{bmatrix} \tag{2.17}$$

2.4.2.3 Constant Power Loads (P)

The load currents are calculated similar to Equation 2.16. The complex phase-to-phase voltage will change on each iteration till convergence is achieved.

Combination of (Z), (I) and (P) loads for both star and delta connections are modeled based on above equations with the percentage effect of each load model.

Since our load flow algorithm use only phase-to-neutral values, all the phase-to-phase voltages and currents must be converted to phase-to-neutral values at the final output. The matrix equation for calculating line current from a delta connected load is given below.

$$\begin{bmatrix} I_a \\ I_b \\ I_c \end{bmatrix} = \begin{bmatrix} 1 & 0 & -1 \\ -1 & 1 & 0 \\ 0 & -1 & 1 \end{bmatrix} . \begin{bmatrix} I_{ab} \\ I_{bc} \\ I_{ca} \end{bmatrix} \tag{2.18}$$

Different types of load models have been discussed in this section, these load models are used in our developed load-flow algorithm. The next section describes about the types three phase transformers and its implementation in the load-flow algorithm.

2.5 Types of three phase transformers

Three phase transformers are one of the major components of radial distribution system. They are found at the substations (known as substation transformers) which change the voltage from transmission (high-voltage) level to distribution (low-voltage level) feeder level. Few transformers are even placed at load ends as per the requirements. The most common type of substation transformer for a three phase four wire system is delta-grounded wye [24] because of its feasibility on the grounded wye side to connect single phase, double phase and three phase loads as per customer requirements.

Four major types of three phase transformers which are generally found on distribution network are modeled in this chapter as follows,

- Delta – Grounded Wye
- Delta – Delta
- Grounded Wye – Grounded Wye
- Grounded Wye – Delta

It is noted that all the transformers are connected according to "American Standard Thirty Degree" connection [25]. This implies that, for a step down connection, the secondary voltage and current leads the primary voltage and current by 30 degrees and for a step – up connection, the secondary voltage and current components leads the primary by 30 degrees.

2.5.1 Transformation matrices and Thevenin equivalent circuit

Before we can proceed to determine the general equations for different types of transformers, it is very important to know the transformation matrices. The below section explains in details about the voltage and current transformation matrices. It also explains the Thevenin equivalent method which is used to model the general equations which are used in the developed load flow analysis.

2.5.1.1 Voltage transformation matrices

The voltage magnitude change between the primary and secondary terminals of the three phase transformers and are defined in terms of turns ratio 'n_t' i.e.

$$n_t = \frac{VLL_{primary}}{VLN_{secondary}} \tag{2.19}$$

The line voltages as a function of turn's ratio and ideal secondary transformer voltages can be given as,

$$[VLL_{ABC}] = [AV] * [Vt_{abc}] \tag{2.20}$$

Where,

$$[AV] = n_t * \begin{bmatrix} 0 & -1 & 0 \\ 0 & 0 & -1 \\ -1 & 0 & 0 \end{bmatrix}$$ (Delta – Wye and Wye – Delta connection)

$$[AV] = n_t * \begin{bmatrix} 1 & 0 & 0 \\ 0 & 1 & 0 \\ 0 & 0 & 1 \end{bmatrix}$$ (Delta – Delta and Wye - Wye connection)

The 30 degree phase change from the primary to secondary side can be obtained by applying the concept of 'theory of symmetrical components'. The three-phase line to line voltages are transformed to sequence voltages by multiplying with $a_s = 1.0\angle 120$. It is given as,

$$[VLL_{012}] = inv(A_s) * [VLL_{ABC}] \tag{2.21}$$

Where, $[A_s] = \begin{bmatrix} 1 & 1 & 1 \\ 1 & a_s^2 & a_s \\ 1 & a_s & a_s^2 \end{bmatrix}$

Now, the relation between the symmetrical component of line voltages and phase voltage is defined as,

$$[VLN_{012}] = [T] * [VLL_{012}] \tag{2.22}$$

Where, $[T] = \begin{bmatrix} 1 & 0 & 0 \\ 0 & t_s^* & 0 \\ 0 & 0 & t_s \end{bmatrix}$ and $t_s = 1.0\angle 30$

From both the above derived sequence components, we can calculate the equivalent phase voltage based on line voltage using the relation as shown below,

$$[VLN_{ABC}] = [W] * [VLL_{ABC}] \tag{2.23}$$

$$[W] = [A_s] * [T] * [A_s]^{-1} = \frac{1}{3} * \begin{bmatrix} 2 & 1 & 0 \\ 0 & 2 & 1 \\ 1 & 0 & 2 \end{bmatrix} \quad (2.24)$$

Similarly, with the knowledge of line to neutral voltage the line to line voltages can be obtained as,

$$[VLL_{ABC}] = [D] * [VLN_{ABC}] \quad (2.25)$$

Where, $[D] = \begin{bmatrix} 1 & -1 & 0 \\ 0 & 1 & -1 \\ -1 & 0 & 1 \end{bmatrix}$

Thus, we have now derived the required voltage transformation matrices which are general and can be used on all types of transformers.

2.5.1.2 Current transformation matrices

The line currents determined here are with reference to the delta currents in a delta type transformer. Only the line-currents are used in load flow analysis.

By applying the Kirchhoff's current law (KCL), the currents flowing through the distribution line can be determined as,

$$[I_{ABC}] = [D][Idelta_{ABC}] \quad (2.26)$$

Where, $[D] = \begin{bmatrix} 1 & -1 & 0 \\ 0 & 1 & -1 \\ -1 & 0 & 1 \end{bmatrix}$

Now, the line currents on the secondary side of transformer with reference to delta currents in the primary side of transformer is given as,

$$[Idelta_{ABC}] = \frac{1}{n_t} * \begin{bmatrix} 1 & 0 & 0 \\ 0 & 1 & 0 \\ 0 & 0 & 1 \end{bmatrix} * [I_{abc}] \quad (2.27)$$

Let, $[AI] = \frac{1}{n_t} * \begin{bmatrix} 1 & 0 & 0 \\ 0 & 1 & 0 \\ 0 & 0 & 1 \end{bmatrix}$

Hence, we have now derived the required general current transformation matrices which can be used on all types of delta connected transformers.

2.5.1.3 Thevenin equivalent circuit

In order to build a generalized model for all the four types of transformers, it is necessary that we use the Thevenin equivalent circuit method.

Let us consider a three bus system with a three phase transformer between bus 2 and 3 as shown in the figure below.

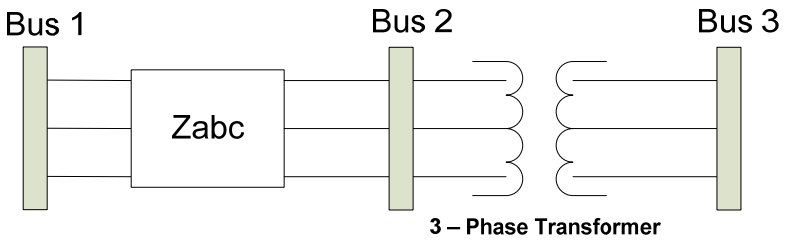

Figure 2.4 Three bus system

The primary side voltage of the transformer can be determined by subtracting the voltage at Bus 1 and the voltage drop on the line 1 – 2. It is given as,

$$[VLN_{ABC2}] = [VLN_{ABC1}] - [Z_{ABC1-2}] * [I_{ABC1-2}] \quad (2.28)$$

The currents on the primary side can be determined with reference to secondary currents by using the following equation,

$$[I_{ABC1-2}] = [Adj_{current}^{xmer}] * [I_{abc2-3}] \quad (2.29)$$

Now, the voltage equation to determine the secondary voltage of the transformer can be formulated as,

$$[VLN_{abc3}] = \left[Adj_{voltage}^{xmer}\right][VLN_{ABC2}] - \left[Adj_{impedance}^{xmer}\right] * [I_{abc2-3}] \quad (2.30)$$

Where,

$[Adj_{current}^{xmer}]$ is termed as 'current adjustment matrix' of the transformer. This matrix is used to relate the three phase currents of secondary side to the primary side of the transformer.

$\left[Adj_{voltage}^{xmer}\right]$ is termed as 'voltage adjustment matrix' of the transformer. This matrix is used to calculate the secondary phasor voltage based on primary phasor voltage of the transformer.

$\left[Adj_{impedance}^{xmer}\right]$ is the 'impedance adjustment matrix' of the transformer. These matrices will be discussed in detail in the next section of this chapter.

By substituting the equations (2.28) and (2.29) in (2.30) we get,

$$[VLN_{abc3}] = \left[Adj_{voltage}\right][VLN_{ABC1}] - (\left[Adj_{voltage}\right] * [Z_{ABC1-2}] * [Adj_{current}] + \left[Adj_{impedance}\right]) * [I_{abc2-3}] \quad (2.31)$$

Now, the Thevenin equivalent voltage is$\left[Adj_{voltage}^{xmer}\right][VLN_{ABC1}]$, the Thevenin equivalent impedance is$(\left[Adj_{voltage}^{xmer}\right] * [Z_{ABC1-2}] * [Adj_{current}^{xmer}] + \left[Adj_{impedance}^{xmer}\right])$.

The impedance adjustment matrix is the three phase impedance matrix of the transformer which is given as $\left[Adj_{impedance}^{xmer}\right] = \begin{bmatrix} \mathrm{Zt_a} & 0 & 0 \\ 0 & \mathrm{Zt_b} & 0 \\ 0 & 0 & \mathrm{Zt_c} \end{bmatrix}$

Where,Zt_a, Zt_b and Zt_c are the equivalent impedance value of the transformer phase a, b and c respectively.

Hence, the developed Thevenin equivalent voltage and impedance matrices are generalized and these equations can be used for all types of transformers.

2.5.2 Delta – Grounded wye connection

A step – down, delta – grounded wye connection is the most popular connection used in distribution networks on a four wire feeder [1]. This is because of the flexibility of connecting single/double or three phase loads at the grounded- wye terminal.

The delta – grounded wye step down connection in a standard thirty degree connection notation is as shown in figure below.

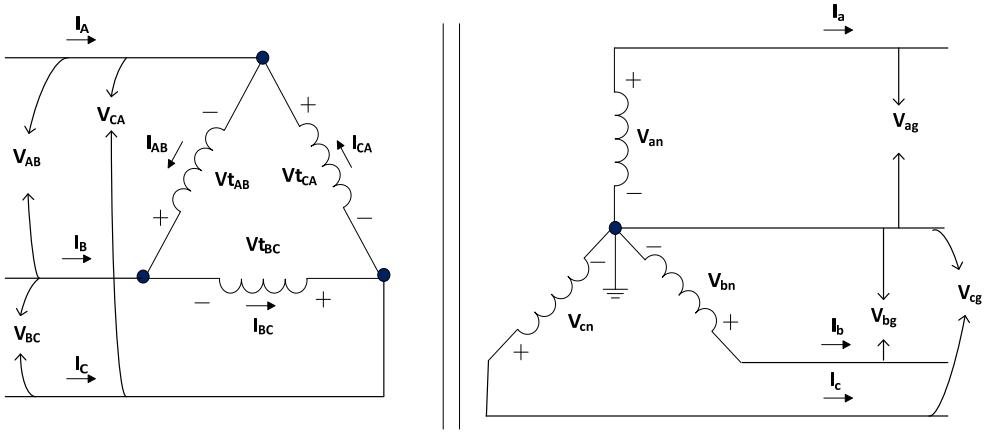

Figure 2.5 Delta – Grounded Wye Transformer

Now, from the transformation matrices and thevenin equivalent we can write the general equations for a delta-grounded wye transformer as,

$$[VLN_{abc}] = \left[Adj_{voltage}^{xmer}\right][VLN_{ABC}] - \left[Adj_{impedance}^{xmer}\right] * [I_{abc}] \quad (2.32)$$

$$[I_{ABC}] = [Adj_{current}^{xmer}] * [I_{abc}] \quad (2.33)$$

Where,

$$\left[Adj_{voltage}^{xmer}\right] = \frac{1}{n_t} * \begin{bmatrix} 1 & 0 & -1 \\ -1 & 1 & 0 \\ 0 & -1 & 1 \end{bmatrix},$$

$$\left[Adj_{impedance}^{xmer}\right] = \begin{bmatrix} Zt_a & 0 & 0 \\ 0 & Zt_b & 0 \\ 0 & 0 & Zt_c \end{bmatrix},$$

$$[Adj_{current}^{xmer}] = \frac{1}{n_t} * \begin{bmatrix} 1 & -1 & 0 \\ 0 & 1 & -1 \\ -1 & 0 & 1 \end{bmatrix},$$

The suffixes “A, B, C” are for primary side and “a, b, c” are for secondary side of transformer.

The above equations are general equation for a standard delta - grounded wye step - down connection.

For delta – grounded wye step-up connection only the adjustment matrices vary and are given as,

$$\left[Adj_{voltage}^{xmer}\right] = \frac{1}{n_t} * \begin{bmatrix} 1 & 0 & -1 \\ 0 & 1 & -1 \\ -1 & 0 & 1 \end{bmatrix}$$

$$\left[Adj_{impedance}^{xmer}\right] = \begin{bmatrix} Zt_a & 0 & 0 \\ 0 & Zt_b & 0 \\ 0 & 0 & Zt_c \end{bmatrix}$$

$$[Adj_{current}^{xmer}] = \frac{1}{n_t} * \begin{bmatrix} 1 & 0 & -1 \\ 0 & 1 & -1 \\ -1 & 0 & 1 \end{bmatrix}$$

2.5.3 Delta – Delta connection

A delta-delta connection is used on a typical three wire delta system. This type of transformer is used mostly to provide service to a three phase delta loads and this connection doesn't have any phase shifts between the primary and secondary terminals of the transformer. Delta-Delta connection transformers are widely implemented at sub-transmission and transmission voltage levels, and rarely used on the distribution side.

The three phase delta – delta connection is as shown in figure below.

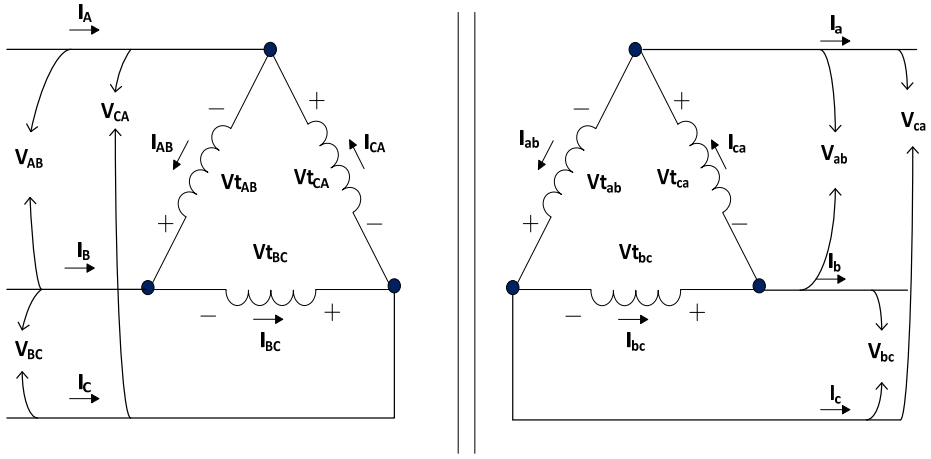

Figure 2.6 Delta – Delta transformer

The equation defining the delta-delta connections are,

$$[VLN_{\text{abc}}] = \left[Adj_{voltage}^{xmer}\right][VLN_{ABC}] - \left[Adj_{impedance}^{xmer}\right] * [I_{abc}] \tag{2.34}$$

$$[I_{\text{ABC}}] = [Adj_{current}^{xmer}] * [I_{abc}] \tag{2.35}$$

Where,

$\left[Adj_{voltage}^{xmer}\right] = [\text{W}] * [\text{AV}]^{-1} * [\text{D}]$

$$\left[Adj_{impedance}^{xmer}\right] = [\mathrm{W}] * \begin{bmatrix} \mathrm{Zt_a} & 0 & 0 \\ 0 & \mathrm{Zt_b} & 0 \\ 0 & 0 & \mathrm{Zt_c} \end{bmatrix} * [\mathrm{D}]$$

$$[Adj_{current}^{xmer}] = \frac{1}{\mathrm{n_t}} * \begin{bmatrix} 1 & 0 & 0 \\ 0 & 1 & 0 \\ 0 & 0 & 1 \end{bmatrix}$$

$$[D] = \begin{bmatrix} 1 & -1 & 0 \\ 0 & 1 & -1 \\ -1 & 0 & 1 \end{bmatrix}$$

The above equations are general equation for a standard step-down and step-up delta-delta connection.

2.5.4 Grounded Wye – Grounded Wye connection

A grounded wye- grounded wye connection is used on a typical four wire multi-grounded system. This type of transformer is used mostly feed multiple loads which are either single phase or three phase loads on a four wire system.

Figure 2.7 show the three phase grounded wye-grounded wye connections.

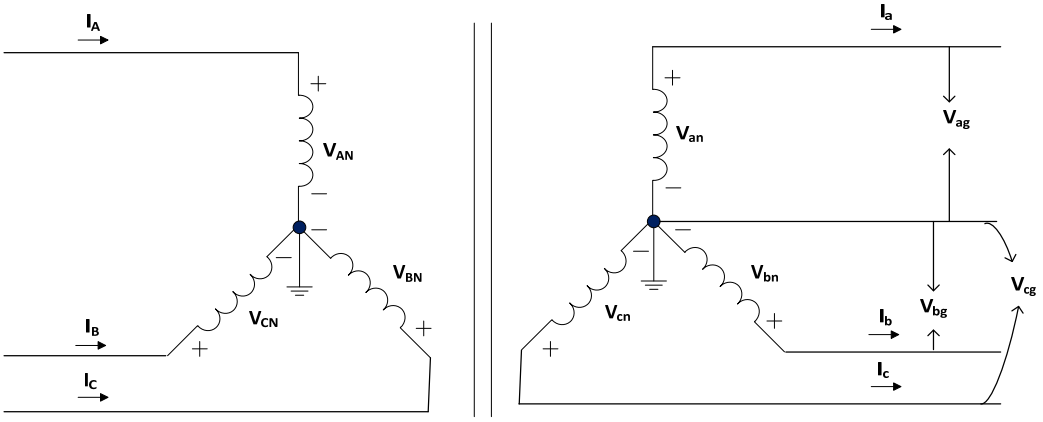

Figure 2.7 Grounded Wye – Grounded Wye transformer

The equation defining the delta-delta connections are,

$$[\mathrm{VLN_{abc}}] = \left[\mathrm{Adj_{voltage}^{xmer}}\right][\mathrm{VLN_{ABC}}] - \left[\mathrm{Adj_{impedance}^{xmer}}\right] * [\mathrm{I_{abc}}] \tag{2.36}$$

$$[\mathrm{I_{ABC}}] = [\mathrm{Adj_{current}^{xmer}}] * [\mathrm{I_{abc}}] \tag{2.37}$$

Where,

$$\left[\mathrm{Adj_{voltage}^{xmer}}\right] = [\mathrm{AV}]^{-1}$$

$$\left[\mathrm{Adj_{impedance}^{xmer}}\right] = \begin{bmatrix} \mathrm{Zt_a} & 0 & 0 \\ 0 & \mathrm{Zt_b} & 0 \\ 0 & 0 & \mathrm{Zt_c} \end{bmatrix}$$

$$[\mathrm{Adj_{current}^{xmer}}] = \frac{1}{\mathrm{n_t}} * \begin{bmatrix} 1 & 0 & 0 \\ 0 & 1 & 0 \\ 0 & 0 & 1 \end{bmatrix}$$

The above derived equations are standard equations for a three phase grounded wye - grounded wye step-down and step-up connection.

2.5.5 Grounded wye – Delta connection

A grounded wye- delta connection is rarely used on a typical four wire grounded system where the load is delta connected. Unlike the other three types of transformers, the analysis of this type of transformer is some-what complicated as the ground impedance on the primary side comes in to play. This creates a problem during the current transformation from the primary to secondary side. In this thesis, the ground resistance is considered to be negligible.

The three phase grounded wye - delta connection is as shown in Figure 2.8.

The equation defining the delta-delta connections are,

$$[VLN_{\mathrm{abc}}] = \left[Adj_{voltage}^{xmer}\right][VLN_{ABC}] - \left[Adj_{impedance}^{xmer}\right] * [I_{abc}] \tag{2.38}$$

$$[I_{\mathrm{ABC}}] = [Adj_{current}^{xmer}] * [I_{abc}] \tag{2.39}$$

Where, $\left[Adj_{voltage}^{xmer}\right] = [\mathrm{W}] * ([\mathrm{AV}]^{-1} - \begin{bmatrix} \mathrm{Zt_a} & 0 & 0 \\ 0 & \mathrm{Zt_b} & 0 \\ 0 & 0 & \mathrm{Zt_c} \end{bmatrix} *$

$$\begin{bmatrix} -1 & -1 & -1 \\ 0 & 0 & 0 \\ \mathrm{n_t} * \mathrm{Zt_c} & \mathrm{n_t} * \mathrm{Zt_c} & \mathrm{n_t} * \mathrm{Zt_c} \end{bmatrix}$$

$$\left[Adj_{impedance}^{xmer}\right] = [\mathrm{W}] * \begin{bmatrix} \mathrm{Zt_a} & 0 & 0 \\ 0 & \mathrm{Zt_b} & 0 \\ 0 & 0 & \mathrm{Zt_c} \end{bmatrix} * \begin{bmatrix} 1 & 0 & 0 \\ -1 & 1 & 0 \\ \mathrm{n_t} * \mathrm{Zt_a} & \mathrm{n_t} * \mathrm{Zt_b} & 0 \end{bmatrix}$$

$$[Adj_{current}^{xmer}] = \frac{1}{\mathrm{n_t}} * \begin{bmatrix} 1 & 0 & 0 \\ 0 & 1 & 0 \\ 0 & 0 & 1 \end{bmatrix} * \begin{bmatrix} 1 & 0 & 0 \\ -1 & 1 & 0 \\ \mathrm{n_t} * \mathrm{Zt_a} & \mathrm{n_t} * \mathrm{Zt_b} & 0 \end{bmatrix}$$

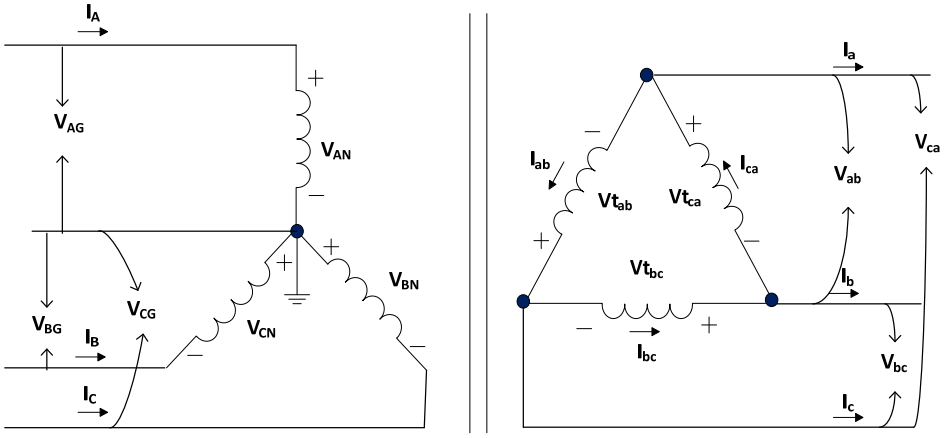

Figure 2.8 Grounded wye – Delta transformer

In this section, the equations are generalized all the four types of three phase transformers. These equations are used for developing the load flow algorithm in this research. The next section explains about the different types of voltage regulators.

2.6 Voltage regulators

Voltage regulation on a three phase radial distribution feeder is a very important function. As the system is radial in nature with only one source i.e. the substation, the voltages at the end of the feeder might not be within the specified value. In such cases, the voltage regulators play an important role by boosting the voltage magnitude to the standard level specified by the distribution system operator.

Below section explains the connection types of a three phase voltage regulators.

2.6.1 Wye connected three-phase voltage regulators

Wye-connected three phase voltage regulator is as shown in Figure 2.9.

The voltage and current equations considering the effective turns ratio of the regulator can be given as,

$$[VLN_{ABC}] = \left[Adj_{voltage}^{regulator}\right] * [VLN_{abc}] \tag{2.40}$$

$$[I_{ABC}] = \left[Adj_{current}^{regulator}\right] * [I_{abc}] \tag{2.41}$$

Where,

$\left[Adj_{voltage}^{regulator}\right] = \left[Adj_{current}^{regulator}\right] = \begin{bmatrix} \frac{1}{a_{R-a}} & 0 & 0 \\ 0 & \frac{1}{a_{R-b}} & 0 \\ 0 & 0 & \frac{1}{a_{R-c}} \end{bmatrix}$, it is the voltage and current adjustment matrix of the wye connected voltage regulator.

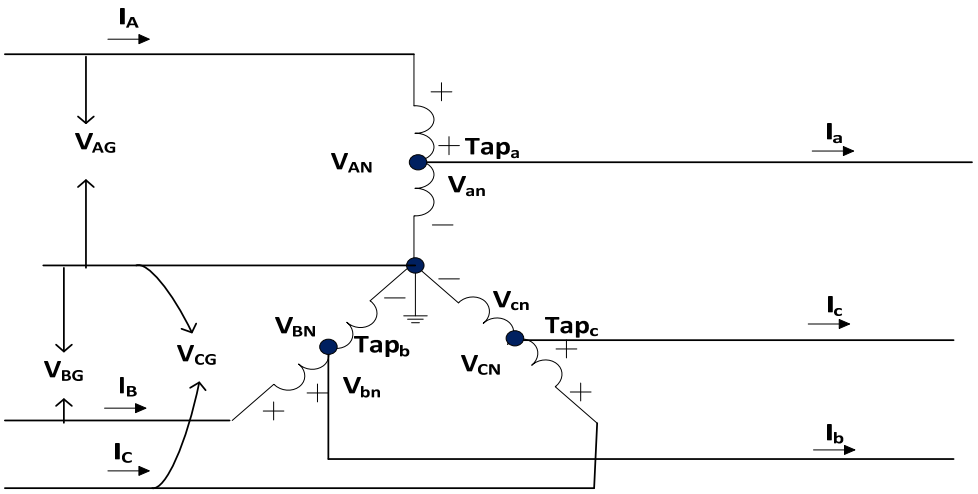

Figure 2.9 Three phase wye connected voltage regulator

According to the American National Standards Institute (ANSI), the turns ratio of the voltage regulator must satisfy a change of voltage from 0.9 p.u to 1.1 p.u in 32 steps. It implies that it must satisfy a voltage change of 0.625% per step.

The effective turns ratio ($a_{R-a}, a_{R-b}, a_{R-c}$) are independent of each other and they are calculated using the following formula.

$$[a_{R-abc}] = \begin{bmatrix} 1 - 0.625\%(Tap_a) & 0 & 0 \\ 0 & 1 - 0.625\%(Tap_b) & 0 \\ 0 & 0 & 1 - 0.625\%(Tap_c) \end{bmatrix} \quad (2.42)$$

The tap settings of the voltage regulator are calculated on a 120 base voltage as,

$$Tap_a = \frac{|120 - |Vload_a||}{0.75}$$

$$Tap_b = \frac{|120 - |Vload_b||}{0.75}$$

$$Tap_c = \frac{|120 - |Vload_c||}{0.75}$$

In most cases the compensator R and X settings will be specified, else they can be computed according to the equation given below.

$$R' + jX' = Rline_{avg} + jXline_{avg}\frac{CT_p}{N_{PT}} \tag{2.43}$$

Where, $N_{PT}\ and\ CT_p$ are the potential and current transformers ratings of the regulator.

2.6.2 Delta connected three-phase voltage regulator

Closed delta connected three-phase voltage regulator is as shown in the Figure 2.10.

The voltage and current equations considering the effective turns ratio of the regulator is as given below. Unlike the wye connection, the equations are not same.

$$[VLL_{\mathrm{ABC}}] = \left[Adj_{voltage}^{regulator}\right] * [VLL_{abc}] \tag{2.44}$$

$$[I_{\mathrm{abc}}] = \left[Adj_{current}^{regulator}\right] * [I_{ABC}] \tag{2.45}$$

Where,

$\left[Adj_{voltage}^{regulator}\right] = \begin{bmatrix} \mathrm{a_{R-ab}} & 1-\mathrm{a_{R-bc}} & 0 \\ 0 & \mathrm{a_{R-bc}} & 1-\mathrm{a_{R-ca}} \\ 1-\mathrm{a_{R-ab}} & 0 & \mathrm{a_{R-ca}} \end{bmatrix}$, it is the voltage adjustment matrix of the regulator in delta connection.

$\left[Adj_{current}^{regulator}\right] = \begin{bmatrix} \mathrm{a_{R-ab}} & 0 & 1-\mathrm{a_{R-ca}} \\ 1-\mathrm{a_{R-ab}} & \mathrm{a_{R-bc}} & 0 \\ 0 & 1-\mathrm{a_{R-bc}} & \mathrm{a_{R-ca}} \end{bmatrix}$, it is the current adjustment matrix of the regulator in delta connection.

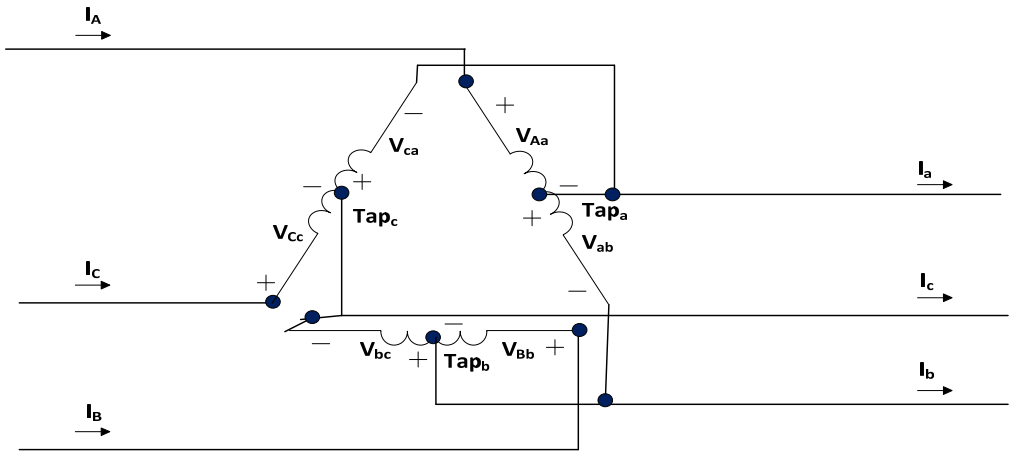

Figure 2.10 Three phase delta connected voltage regulator

According to the American National Standards Institute (ANSI), the turns ratio of the voltage regulator must satisfy a change of voltage from 0.9 p.u to 1.1 p.u in 32 steps. It implies that it must satisfy a change of 0.625% per step.

From the above equation it is difficult to apply a delta connected regulator for power flow analysis as the effective turns ratio ($a_{R-a}, a_{R-b}, a_{R-c}$) are dependent on each other.

The turns ratio and the compensator setting calculations of the regulator are similar to wye connected regulator.

The equations modeled for both types of voltage regulator are used in our load flow algorithm. Next section describes about the modeling of shunt capacitor banks and their effect on a three phase distribution network.

2.7 Shunt capacitors

Shunt capacitors are one of the important components used in power distribution systems. They help to reduce the losses, provide reactive power and also used for voltage regulation. These shunt capacitors can be connected in three phase, two phase or single phase connection types in either delta or wye fashion.

2.7.1 Wye connected shunt capacitors

The three phase wye connected capacitor banks is as shown in the Figure 2.11.

In general, the values of capacitor units either single-phase or three-phase are specified in kVAr and kV. From these kVAr and kV values, the susceptances of the capacitor bank are calculated in Siemens (S) [2] using the formula given below,

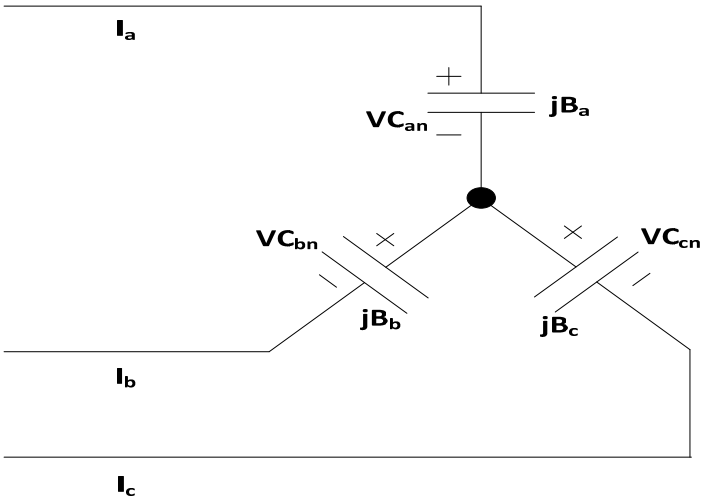

Figure 2.11 Wye – connected capacitor bank

$$\mathrm{B_{phase}} = \frac{\mathrm{KVAr}}{\mathrm{KV_{LN}^2 * 1000}}\,\mathrm{S} \tag{2.46}$$

The line current of the capacitor banks are given as,

$$\begin{bmatrix} IC_a \\ IC_b \\ IC_c \end{bmatrix} = \begin{bmatrix} jB_a \\ jB_b \\ jB_c \end{bmatrix} . \begin{bmatrix} V_{an} \\ V_{bn} \\ V_{cn} \end{bmatrix} \tag{2.47}$$

2.7.2 Delta connected shunt capacitors

The three phase delta connected capacitor banks is as shown in the Figure 2.12.

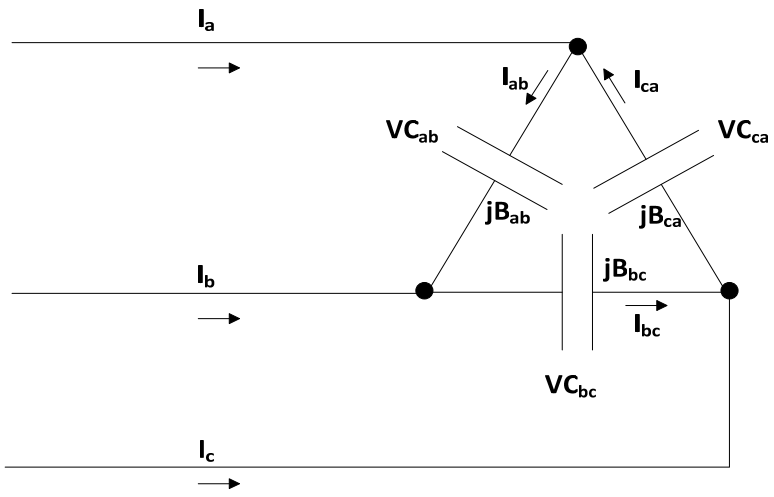

Figure 2.12 Delta connected capacitor bank

Similar to wye-connected capacitor bank, the susceptances of the delta connected capacitors are calculated from the specified kVAr and kV rating using the equation given below.

$$B_{phase} = \frac{KVAr}{KV_{LL}^2 * 1000} S \tag{2.48}$$

The delta current of the capacitor banks are given as,

$$\begin{bmatrix} \mathrm{IC_{ab}} \\ \mathrm{IC_{bc}} \\ \mathrm{IC_{ca}} \end{bmatrix} = \begin{bmatrix} \mathrm{jB_a} \\ \mathrm{jB_b} \\ \mathrm{jB_c} \end{bmatrix} . \begin{bmatrix} \mathrm{V_{ab}} \\ \mathrm{V_{bc}} \\ \mathrm{V_{ca}} \end{bmatrix} \tag{2.49}$$

The delta currents of the capacitor banks are transformed in to line currents using the following relation,

$$\begin{bmatrix} IC_a \\ IC_b \\ IC_c \end{bmatrix} = \begin{bmatrix} 1 & 0 & -1 \\ -1 & 1 & 0 \\ 0 & -1 & 1 \end{bmatrix} \begin{bmatrix} IC_{ab} \\ IC_{bc} \\ IC_{ca} \end{bmatrix} \tag{2.50}$$

The above developed equations for shunt capacitor banks can be used in all types of load flow algorithms. The effect of switches and its implementation in the load flow algorithm is explained in the next section.

2.8 Switches

The switches on the distribution networks are modeled as a branch matrix termed as ‘switch branch matrix’ with zero impedance but with switch status which is either 1 or 0.

$$\begin{bmatrix} V_a^{k+1} \\ V_b^{k+1} \\ V_c^{k+1} \end{bmatrix} = \begin{bmatrix} S_{on} & 0 & 0 \\ 0 & S_{on} & 0 \\ 0 & 0 & S_{on} \end{bmatrix} \begin{bmatrix} V_a^k \\ V_b^k \\ V_c^k \end{bmatrix} \tag{2.51}$$

$$\begin{bmatrix} I_a^{k+1} \\ I_b^{k+1} \\ I_c^{k+1} \end{bmatrix} = \begin{bmatrix} S_{on} & 0 & 0 \\ 0 & S_{on} & 0 \\ 0 & 0 & S_{on} \end{bmatrix} \begin{bmatrix} I_a^k \\ I_b^k \\ I_c^k \end{bmatrix} \tag{2.52}$$

Where, S_{on} is switch status on i.e. $S_{on} = 1$, S_{off} is switch status off i.e. $S_{off} = 0$ and k is the iteration number.

Equations for all the network parameters and system components models have been developed in the above sections 2.2 – 2.8. These models and equation will be used in our developed load flow algorithm which is explained in detail in the next section.

2.9 Load flow algorithm

One of the main aspects of distribution system analysis is load flow studies. Load flow analysis will result in accurate determination of node voltages, phase angles, line flows in kW and kVAr, power losses in each line, total power loss in a given system etc. [10].

Sections 2.2-2.8 explained about modeling of different components of a typical power distribution system, these models will be used in the load flow analysis in steady state condition.

Similar to transmission system analysis, the available information are the complex bus voltages at the substation or source which is 1.0 p.u. in most cases, load types (Z, I, P) and complex power drawn by all the loads. When analyzing a typical existing case, the phase impedance models and transformer models are also specified prior to analysis, else for a new design, the phase impedance models are to be calculated using Carson's equations and Kron's reduction technique as explained in section 2.3.

In this study, we have considered an existing IEEE test feeder, hence all the required information required for analysis is provided in [26] - [28].

The proposed algorithm is based on two main matrices viz. bus injection to branch current matrix (BIBC) and branch current to bus voltage matrix (BCBV). These two matrices take full advantage of the distribution network topology for load flow.

The method of using the BIBC and BCBV matrices for load flow was first introduced by J.H. Teng [29]. However his research did not include any method to include the different types of three phase transformers, shunt capacitance, switch status etc. In this research, we have introduced few additional adjustment matrices along with BIBC and BCBV which can incorporate all the network components, hence resulting in a comprehensive load flow solution.

2.9.1 Development of bus-injection to branch-current (BIBC) matrix

The BIBC matrix represents the relation between current injections at a particular bus to the sum of currents in the associated branch.

2.9.1.1 Algorithm development

In order to understand the formation of BIBC matrix, a simple modified IEEE 4-bus distributed network is used as shown in the Figure 2.13.

Initially, all the complex power injections at the buses are converted into complex current injection by using the Equation 2.54.

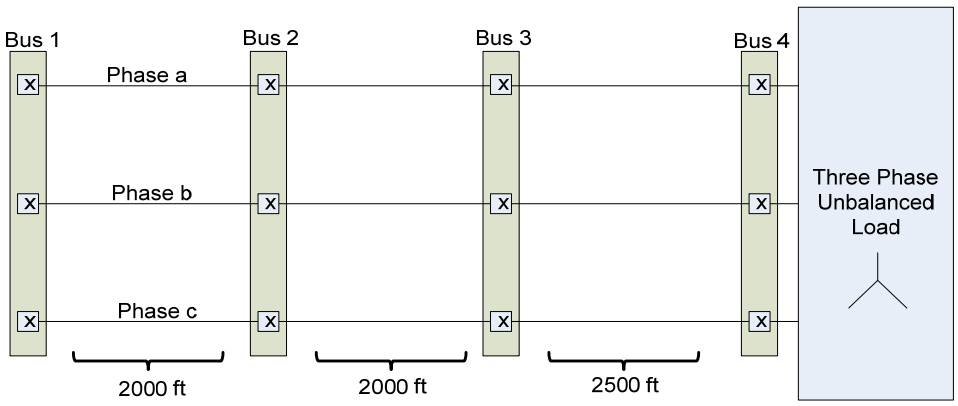

Figure 2.13 Modified IEEE-4 bus test feeder

$$S_i = P_i + jQ_i \tag{2.53}$$

$$I_i^k = \left[\frac{P_i + jQ_j}{V_i^k}\right]^* \tag{2.54}$$

Where, i = 1 ….. no. of buses (n) and k is the iteration number.

Now, after obtaining the bus current injections at every bus, using the Kirchhoff's Current Law (KCL) the relationship between branch currents and bus current injections are calculated. We know that, the algebraic sum of the associated bus current injections will result in the current flow through that particular branch. It is as shown in the below example,

For Branch 1 (B_1)

$$B_1^a = I_2^a + I_3^a + I_4^a \tag{2.55}$$

$$B_1^b = I_2^b + I_3^b + I_4^b \tag{2.56}$$

$$B_1^c = I_2^c + I_3^c + I_4^c \tag{2.57}$$

Where,

I_2^a, I_2^b, I_2^c are current injections at bus 2 and of phases a, b and c respectively.

I_3^a, I_3^b, I_3^c are current injections at bus 3 and of phases a, b and c respectively.

I_4^a, I_4^b, I_4^c are current injections at bus 4 and of phases a, b and c respectively.

Similarly for branch 2 (B_2) and branch 3 (B_3)

$$B_2^a = I_3^a + I_4^a \tag{2.58}$$

$$B_3^a = I_4^a \tag{2.59}$$

The above equations can be represented in matrix form as,

$$\begin{bmatrix} B_1^p \\ B_2^p \\ B_3^p \end{bmatrix} = \begin{bmatrix} 1 & 1 & 1 \\ 0 & 1 & 1 \\ 0 & 0 & 1 \end{bmatrix} \begin{bmatrix} I_2^p \\ I_3^p \\ I_4^p \end{bmatrix} \tag{2.60}$$

Where, 'p' is the corresponding phase (a, b, or c).

The above Equation 2.58 can be expressed in simplified form as,

$$[B_m^p] = [BIBC][I_n^p] \tag{2.61}$$

Where, m is branch number, n is bus number and BIBC is bus-injection to branch-current matrix.

As observed in (2.60), the BIBC contains only 0 and 1 and it is an upper triangular matrix. This can be easily expanded for multi-phase system, i.e. for a typical three phase system, B_1^p and I_2^p will be a 3x1 vector, 3x3 identity matrix and 3x3 zero matrix will be replaced in the one's and zero's of the BIBC matrix.

2.9.1.2 BIBC formation procedure for an n-bus distribution system

The flow chart in Figure 2.14 shows the procedure to build the BIBC matrix for a multi-phase n- bus distribution network.

2.9.2 Development of branch-current to bus-voltage (BCBV) matrix

The relation between the branch currents and the bus voltages of a distribution network is represented by the BCBV matrix.

2.9.2.1 Algorithm development

For the modified IEEE 4 bus system, the bus voltages and branch currents relationship is expressed as,

$$V_2^p = V_1^p - B_1^p Z_{12}^{abc} \tag{2.62}$$

$$V_3^p = V_2^p - B_2^p Z_{23}^{abc} \tag{2.63}$$

$$V_4^p = V_3^p - B_3^p Z_{34}^{abc} \tag{2.64}$$

Now, substituting the equations (2.60) and (2.61) in (2.62) we get,

$$V_4^p = V_1^p - B_1^p Z_{12}^{abc} - B_2^p Z_{23}^{abc} - B_3^p Z_{34}^{abc} \tag{2.65}$$

Therefore, from Equation (2.63), we can see that any bus voltage is a function of substation/source voltage, line impedance and corresponding branch currents, hence the relation between branch current and bus voltage can be expressed in matrix form as,

$$\begin{bmatrix} V_1^p \\ V_1^p \\ V_1^p \end{bmatrix} - \begin{bmatrix} V_2^p \\ V_3^p \\ V_4^p \end{bmatrix} = \begin{bmatrix} Z_{12}^{abc} & 0 & 0 \\ Z_{12}^{abc} & Z_{23}^{abc} & 0 \\ Z_{12}^{abc} & Z_{23}^{abc} & Z_{34}^{abc} \end{bmatrix} \begin{bmatrix} B_1^p \\ B_2^p \\ B_3^p \end{bmatrix} \tag{2.66}$$

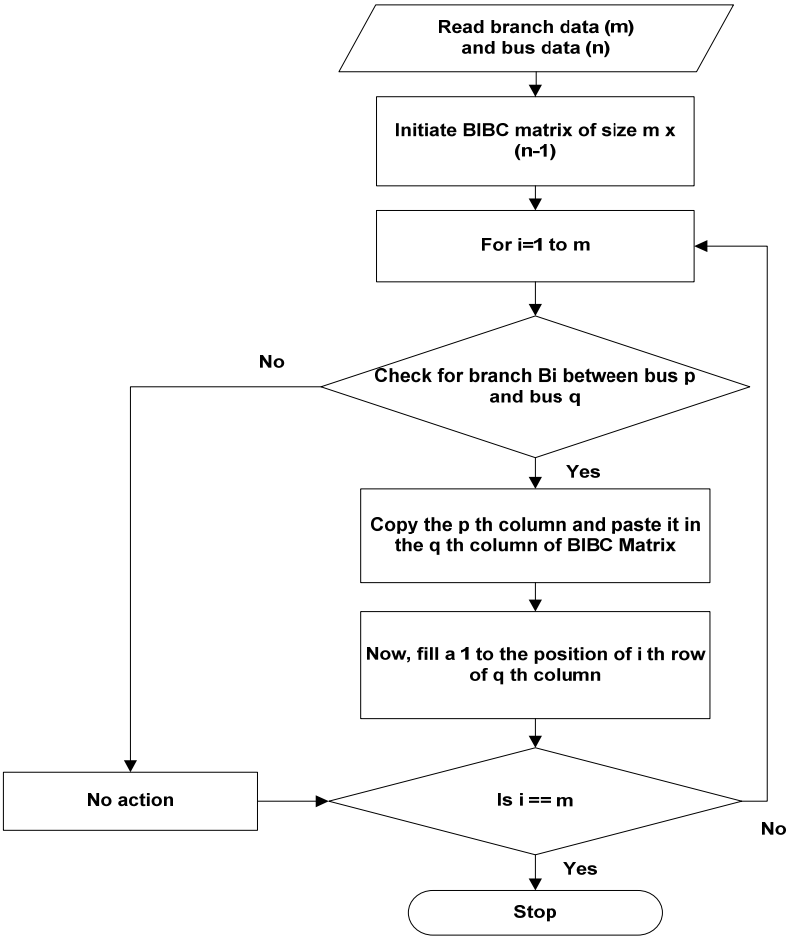

Figure 2.14 Flow chart for BIBC matrix formation

Where,Z_{12}^{abc},Z_{23}^{abc}, Z_{34}^{abc} are the phase impedance value of the lines 1-2, 2-3 and 3-4 respectively.

The above Equation (2.64) can be expressed as,

$$[\Delta V_{1,n}^{p}] = [BCBV][B_{m}^{p}] \tag{2.67}$$

Where 'm' is branch number, 'n' is bus number and 'p' is the corresponding phase,

2.9.2.2 BCBV formation procedure for an n-bus distribution system

The following flow chart shows the procedure to build the BCBC matrix for a multi-phase n- bus distribution network.

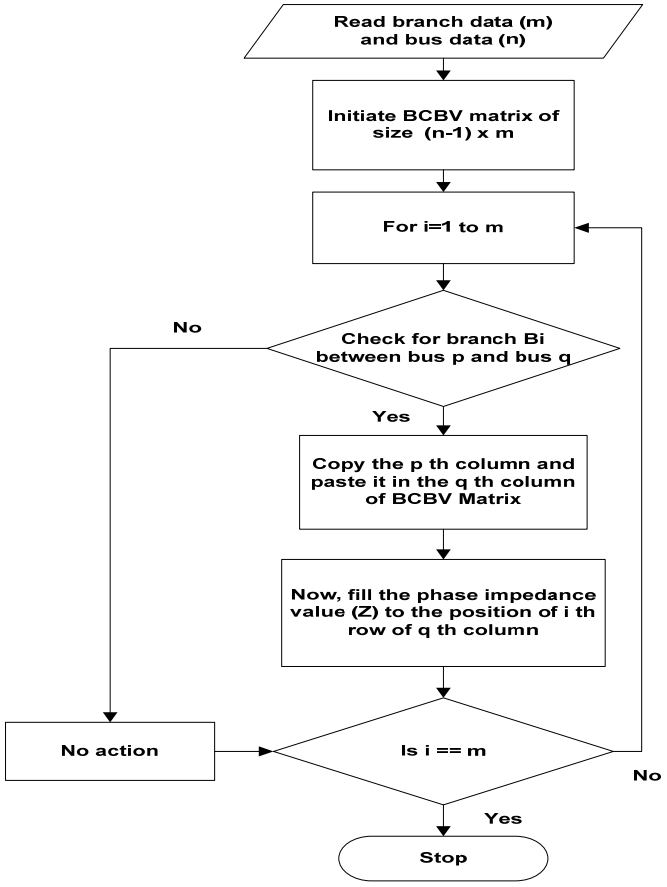

Figure 2.15 Flow chart for BCBV matrix formation

2.9.3 Adjustment matrix

The method explained in the above section did not consider the effects of network components, and it was assumed the line to be three phase overhead lines with three phase loads constant power loads. For accurate analysis of distribution system it is necessary to consider the effects of all the major distribution system parameters. In this section we will introduce few adjustment matrices as a function related with the existing BIBC and BCBV matrices. These adjustment matrices will assimilate all the network

components such as four major types of three phase transformers, shunt capacitance, three phase overhead lines and underground cables and different types of load.

The adjustment matrices for the above mention network components are already developed in sections 2.2 - 2.8. These developed adjustment matrices can be directly used in the load flow analysis by improvising the BCBV and BIBC matrices. It is illustrated in the following section.

2.9.3.1 Improvisation of BCBV matrix

We know that, the BCBV matrix contains the impedances of all the three phase line segments. Hence anything which is related to impedance or its corresponding voltage, that particular section of BCBV will be modified.

Let us consider the IEEE-4 bus test feeder with a three phase delta - grounded wye transformer between bus 2 and bus 3. The test system is being modified by placing a switch between bus 1 and 2 and a voltage regulator at bus 4 as shown in the Figure 2.16. A three phase wye - connected capacitor bank was also placed at bus 4. This example takes into consideration of all the major network components.

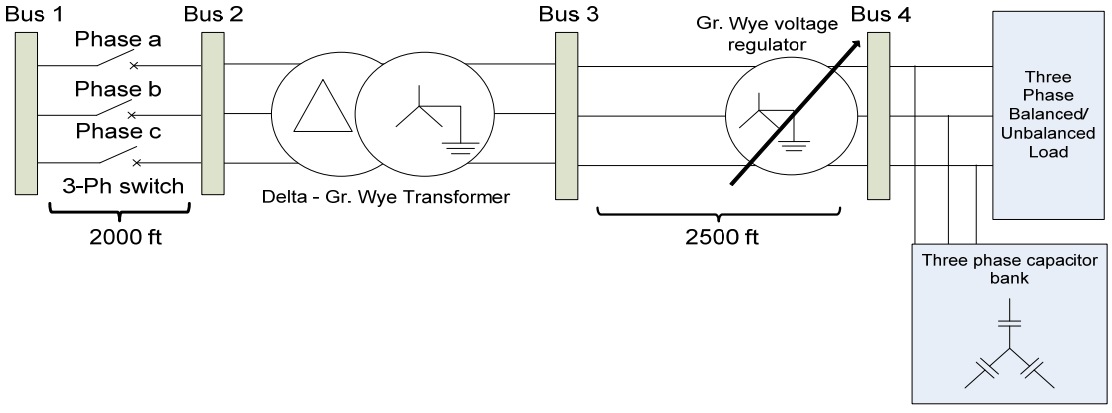

Figure 2.16 Comprehensive IEEE 4- bus Network – modified

Now, considering the voltage adjustment matrices of the transformer, voltage regulator and switch as derived in the above sections the bus voltage equations can be formulated as,

$$V_2^p = S_{on} V_1^p - Z_{12}^{abc} B_1^p \tag{2.68}$$

$$V_3^p = Adj_{voltage}^{xmer} V_2^p - Z_{tr}^{abc} B_2^p \tag{2.69}$$

$$V_4^p = Adj_{voltage}^{regulator} V_3^p - Z_{34}^{abc} B_3^p \tag{2.70}$$

Now, substituting the equations (2.68) and (2.69) in (2.70) we get,

$$V_4^p = S_{on} Adj_{voltage}^{xmer} Adj_{voltage}^{regulator} V_1^p - Adj_{voltage}^{xmer} Adj_{voltage}^{regulator} B_1^p Z_{12}^{abc} - Adj_{voltage}^{regulator} B_2^p Z_{23}^{abc} - Adj_{voltage}^{regulator} B_3^p Z_{34}^{abc} \tag{2.71}$$

Therefore, from Equation (2.71), we can see that any bus voltage is a function of substation voltage, line impedance, corresponding branch currents, transformer adjustment matrix and voltage regulator adjustment matrix. Hence a generalized relation between branch current and bus voltage can be expressed in matrix form as,

$$\begin{bmatrix} S_{on} & 0 & 0 \\ 0 & S_{on} & 0 \\ 0 & 0 & S_{on} \end{bmatrix} * \left(\begin{bmatrix} 1 \\ 1 \\ Adj_{voltage}^{regulator} \end{bmatrix} . \begin{bmatrix} 1 \\ Adj_{voltage}^{xmer} \\ Adj_{voltage}^{xmer} \end{bmatrix} . \begin{bmatrix} V_1^p \\ V_1^p \\ V_1^p \end{bmatrix} \right) - \begin{bmatrix} V_2^p \\ V_3^p \\ V_4^p \end{bmatrix} =$$

$$\left(\begin{bmatrix} Z_{12}^{abc} & 0 & 0 \\ Z_{12}^{abc} & Z_{tr}^{abc} & 0 \\ Z_{12}^{abc} & Z_{tr}^{abc} & Z_{34}^{abc} \end{bmatrix} . \begin{bmatrix} 1 & 1 & 1 \\ Adj_{voltage}^{xmer} & 1 & 1 \\ Adj_{voltage}^{xmer} & 1 & 1 \end{bmatrix} . \begin{bmatrix} 1 & 1 & 1 \\ 1 & 1 & 1 \\ Adj_{voltage}^{regulator} & Adj_{voltage}^{regulator} & Adj_{voltage}^{regulator} \end{bmatrix} \right) \begin{bmatrix} B_1^p \\ B_2^p \\ B_3^p \end{bmatrix}$$

(2.72)

The above equation (2.72) can be simplified as,

$$[S_b] * \left(\left[Adj_{voltage}\right].\left[V_1^p\right]\right) - \left[V_n^p\right] = \left([BCBV].\left[Adj_{impedance}\right]\right) * \left[B_m^p\right]_{improved} \quad (2.73)$$

Where,

'm' is branch number,

'n' is bus number,

'p' is the corresponding phase.

$\left[Adj_{voltage}\right]$ and $\left[Adj_{impedance}\right]$ are voltage adjustment matrix and impedance adjustment matrix respectively due to the effect of transformer and voltage regulator, $[S_b]$ is the branch switch matrix.

The above equation can be further simplified as,

$$\left[V_1^p\right]_{improved} - \left[V_n^p\right] = [BCBV]_{improved} * \left[B_m^p\right]_{improved} \quad (2.74)$$

2.9.3.2 Improvisation of BIBC matrix

We know that, the BIBC matrix contains only ones and zeros of all the three phase branch segments connecting each other. Continuing the above example and considering the current adjustment matrices of transformer, voltage regulator, capacitor bank and branch switch status matrix as derived in the above sections the branch current equations can be formulated as,

$$B_1^p =$$

$$S_{on}\left(\left(I_2^p + I_{2sc}^p\right) + Adj_{current}^{regulator}\left(I_3^p + I_{3sc}^p\right) + Adj_{current}^{xmer} Adj_{current}^{regulator}\left(I_4^p + I_{4sc}^p\right)\right) \quad (2.75)$$

$$B_2^p = S_{on}\left(\left(I_3^p + I_{3sc}^p\right) + Adj_{current}^{regulator}\left(I_4^p + I_{4sc}^p\right)\right) \quad (2.76)$$

$$B_3^p = S_{on}\left(I_4^p + I_{4sc}^p\right) \quad (2.77)$$

The relationship can be represented in matrix form as,

$$\begin{bmatrix} B_1^p \\ B_2^p \\ B_3^p \end{bmatrix} =$$

$$\begin{bmatrix} \mathrm{S_{on}} & 0 & 0 \\ 0 & \mathrm{S_{on}} & 0 \\ 0 & 0 & \mathrm{S_{on}} \end{bmatrix} \left(\begin{bmatrix} 1 & 1 & 1 \\ 0 & 1 & 1 \\ 0 & 0 & 1 \end{bmatrix} . \begin{bmatrix} 1 & 1 & Adj_{current}^{xmer} \\ 1 & 1 & 1 \\ 1 & 0 & 1 \end{bmatrix} . \begin{bmatrix} 1 & Adj_{current}^{regulator} & Adj_{current}^{regulator} \\ 1 & 1 & Adj_{current}^{regulator} \\ 1 & 0 & 1 \end{bmatrix} \right) *$$

$$\begin{bmatrix} \left(I_2^p + I_{2sc}^p\right) \\ \left(I_3^p + I_{3sc}^p\right) \\ \left(I_4^p + I_{4sc}^p\right) \end{bmatrix} \quad (2.78)$$

The above Equation (2.76) can be simplified as,

$$\left[B_m^p\right] = [S_b] * \left([BIBC].\left[Adj_{current}^{xmer}\right].\left[Adj_{current}^{reg}\right]\right) * \left[\left(I_n^p + I_{nsc}^p\right)\right] \quad (2.79)$$

Where,

'm' is branch number,

'n' is bus number,

$[Adj_{current}^{xmer}]$ and $\left[Adj_{current}^{regulator}\right]$ are the vector product of current adjustment matrix of transformer and voltage regulator respectively,

$[S_b]$ is the branch switch status matrix.

I_{nsc}^p is the current from shunt capacitor banks connected at bus 'n' and phase 'p'

The above equation can be further simplified as,

$$\left[B_m^p\right]_{improved} = [BIBC]_{improved} * \left[\left(I_n^p + I_{nsc}^p\right)\right] \quad (2.80)$$

2.9.4 Load flow Solution Technique

After developing the BIBC (improved), BCBV (improved) and Adjustment Matrices based on the topology, network components and line parameters of a radial distribution system, the correlation between the bus current injections and bus voltages can be formulated as,

$$\left[V_1^p\right]_{improved} - \left[V_n^p\right] = [BCBV]_{improved}[BIBC]_{improved}\left[\left(I_n^p + I_{nsc}^p\right)\right] \quad (2.81)$$

$$\left[V_1^p\right]_{improved} - \left[V_n^p\right] = [DLF]_{improved}\left[\left(I_n^p + I_{nsc}^p\right)\right] \quad (2.82)$$

Where $[DLF]_{improved} = [BCBV]_{improved} * [BIBC]_{improved}$

Now, by iteratively solving the Equations (2.83) - (2.85) we can determine the load flow solution for radial power distribution network.

$$I_n^{pk} = (P_n^p + jQ_n^p / V_n^{pk})^* \quad (2.83)$$

$$\left[\left[V_1^p\right]_{improved} - \left[V_n^p\right]^{k+1}\right] = [DLF]_{improved}\left[\left(I_n^p + I_{nsc}^p\right)^k\right] \quad (2.84)$$

$$\left[V_n^{pk+1}\right] = \left[V_1^p\right]_{improved} - \left[\left[V_1^p\right]_{improved} - \left[V_n^p\right]^{k+1}\right] \quad (2.85)$$

Where, V_1^p is the substation voltage and k is the iteration number.

From Equation (2.83), we calculate the current injection at k^{th} iteration; the obtained current injection value is used to determine the voltage difference as shown in Equation (2.84) and these voltages are improved during every iteration by using the Equation (2.85). Consequently the complex phasor bus voltages and currents can be obtained after k iterations.

CHAPTER III

STATIC STATE ESTIMATION FOR A THREE-PHASE UNBALANCED RADIAL POWER DISTRIBUTION NETWORKS

3.1 Introduction

This chapter provides a detail description about a static state estimation algorithm for a three phase unbalanced radial power distribution network based on weighted least squares (WLS) approach. The WLS method will be explained in the following sections. This developed algorithm will select a minimum number of best suitable measurements without compromising the observability and calculates a good estimate for the system. The proposed algorithm also includes load modeling, which is very crucial parameter for obtaining a good estimate of state variables [20]. This method can be directly applied to any of the existing three phase power distribution system. The real time data from the SCADA/RTU's will be utilized to estimate the operating state, but in this research the results obtained from the load flow method will be used as measurement values to estimate the state variables of the three phase distribution systems.

Measurement devices and remote terminal units such as potential transformer for voltage measurement, current transformer for ampere measurement, real and reactive power measurement, phasor measurement units (PMS), circuit breaker status etc., cannot be directly connected to the Energy Management system (EMS) or the topology processor, the data obtained must be processed by the state estimator and its output is

utilized by the EMS [13]. In general, the state estimator receives all the data in real time and relates it with the corresponding equations which are formulated based on network topology and filters the errors in the measurement. This filtered data is utilized by the EMS and other devices in order to ascertain the operating state of the power system.

During the latter part of 20^{th} century, state estimation algorithms were much focused and applied on power transmission systems [30]. This was possible because of the availability of measurement data and economic feasibility to install measuring units as transmission system analysis was very predominant. Now-a-days with the growth of smart grids and micro grid concepts, the availability of data from smart meters installed at the medium level voltage to low level voltage distribution systems are abundant [15], when compared to previous years i.e. during 1980's on the analysis of power distribution system.

By considering this available abundant data, state estimation procedure has been applied to a three phase power distribution network. With an increase in electrical energy demand, and huge expansion of distribution feeders, the analysis of distribution system has become important and so as the state estimation [14] and [16].

As a part of this research, we have incorporated two important techniques which will help to increase the state estimation accuracy and also reduce the computational time. One of them is the load modeling technique (LMT) and the other one is observability analysis based measurement selection technique (OA-MST). Since the three-phase distribution network consists of different types of loads as explained in chapter 2. To calculate an accurate estimate of state variables, the effects of each type of load models are to be considered in the SE algorithm. As explained in the before

paragraph, the data available from the automated distribution system is assumed to be abundant and hence the system is observable, but it is not required to process all the available data to get a good estimate. Our algorithm scans all the available data and selects the predefined data set based on meter variance factor (V.F.) and meter importance factor (I.F.) of the measurement without compromising the observability of the system. By doing so, the accuracy of the state variables obtained is greatly enhanced and the computation time is considerably reduced.

3.2 State estimation procedure

The values obtained from the measurement devices may be deprived of accuracy due to communication error, presence of bad data etc. Due to these errors the mathematical model of state estimation is represented with an error as shown below,

$$Z_i = \hat{Z}_i + e_i \tag{3.1}$$

Where, Z_i is the measured value, $\hat{Z}_i$ is the estimated measurement value, e_i is the possible measurement error of the device and the suffix 'i' ranges from 1 to number of measurement units.

Equation (3.1) can also be represented as a function of state variable as shown below,

$$Z_i = h_i(x) + e_i \tag{3.2}$$

Where, $\hat{Z}_i = h_i(x)$ and $h_i(x)$ is a vector of nonlinear functions.

An example is illustrated below, let us assume that the real and reactive powers flow between bus i and bus j are being measured, the equations for line flows can be determined as,

$$P_{ij} = |V_i||V_j||Y_{ij}|\cos(\delta_{ij} + \theta_{ij}) - |V_i|^2|Y_{ij}|\cos(\theta_{ij}) \quad (3.3)$$

$$Q_{ij} = |V_i||V_j||Y_{ij}|\sin(\delta_{ij} + \theta_{ij}) - |V_i|^2|Y_{ij}|\sin(\theta_{ij}) \quad (3.4)$$

According to state estimation formulation as shown in (3.2), if P_{ij} and Q_{ij} are considered to be measurement vectors then it can be represented as,

$$\begin{bmatrix} P_{ij} \\ Q_{ij} \end{bmatrix} = \begin{bmatrix} |V_i||V_j||Y_{ij}|\,cos(\delta_{ij} + \theta_{ij}) - |V_i|^2|Y_{ij}|\,cos(\theta_{ij}) \\ |V_i||V_j||Y_{ij}|\,sin(\delta_{ij} + \theta_{ij}) - |V_i|^2|Y_{ij}|\,sin(\theta_{ij}) \end{bmatrix} + \begin{bmatrix} e_{P_{ij}} \\ e_{Q_{ij}} \end{bmatrix} \quad (3.5)$$

Where,

$|V_i|$ is the voltage magnitude at bus 'i',

$|V_j|$ is the voltage magnitude at bus 'j',

$|Y_{ij}|$ is the admittance between bus 'i' and bus 'j',

δ_{ij} is the voltage angle between bus 'i' and bus 'j',

θ_{ij} is the admittance angle between bus 'i' and bus 'j',,

$e_{P_{ij}}$and $e_{Q_{ij}}$are the corresponding real and reactive power measurement errors respectively.

The above format represents the measurement function in terms of network variables which are assumed to be known with zero mean Gaussian noise and the bus voltages and phase angels form the state variables. This is solved for convergence of the state variables using weighted least squares method.

3.3 Weighted least square method

Weighted least squares method is one of the most common approach for solving a state estimation problem [19] and [31]. This method follows an iterative procedure to obtain a solution for any given state estimation problem. The convergence of this method

is achieved by minimizing the performance index or the objective function $'J(x)'$ (by identifying the best state variable which is used to minimize it). $'J(x)'$ is termed as the weighted sum of square errors and is given as,

$$J(x) = \sum_{i=1}^{n} (Z_i - h_i(x))^2 / R_{ii} \tag{3.6}$$

Eq. (3.6) can also be represented in matrix notation as,

$$J(x) = [Z_i - h_i(x)]^T [R]^{-1} [Z_i - h_i(x)] \tag{3.7}$$

Where R is the inverse of weighting factor, it is also termed as the diagonal covariance matrix of the measurement and it is represented in (3.8).

As shown in Eq. (3.7), the inverse of the measurement covariance matrix determine the weights of the system, this implies that higher quality of measurement have smaller covariance value when compared to measurements with low or poor quality, which has higher covariance values.

$$R = \begin{bmatrix} \sigma_1^2 & 0 & 0 & 0 & 0 \\ 0 & \sigma_2^2 & 0 & 0 & 0 \\ 0 & \vdots & \ddots & \cdots & 0 \\ 0 & 0 & 0 & \sigma_{n-1}^2 & 0 \\ 0 & 0 & 0 & 0 & \sigma_n^2 \end{bmatrix} \tag{3.8}$$

The WLS method focuses of minimizing the objective function J(x) which is given by (3.7). In order to minimize J(x), the first order partial differentiation (necessary) condition must hold good, i.e. the equation (3.9) must be satisfied. The solution is briefed as follows,

$$f(x) = \frac{\partial J(x^k)}{\partial x} = 0 \tag{3.9}$$

Solving the performance index $J(x)$ results in the following equation,

$$f(x) = \frac{\partial J(x^k)}{\partial x} = -H^T(x^k)R^{-1}(Z - h(x^k)) = 0 \tag{3.10}$$

Where, $H(x^k)$ is the measurement Jacobian matrix is evaluated at k^{th} iteration and is given as,

$$H(x^k) = \left[\frac{\partial h(x^k)}{\partial x}\right] = \begin{bmatrix} \frac{\partial h_1}{\partial x_1} & \frac{\partial h_1}{\partial x_2} & \cdots & \frac{\partial h_1}{\partial x_n} \\ \vdots & \cdots & \ddots & \vdots \\ \frac{\partial h_m}{\partial x_1} & \frac{\partial h_m}{\partial x_2} & \cdots & \frac{\partial h_m}{\partial x_n} \end{bmatrix} \tag{3.11}$$

The above non-linear function $f(x)$ is expanded using Taylors series as shown below.

$$f(x) = f(x^k) + \Delta x^k \frac{\partial f(x^k)}{\partial x} + \cdots = 0 \tag{3.12}$$

The obtained equation neglecting the higher order terms can be solved by iterative Gauss-Newton method. As power system equations are mostly nonlinear in nature, it can be solved only by iteration process. Hence at the $(k+1)^{th}$ iteration, the refreshed values of the states are updated using the following relation,

$$x^{k+1} = x^k - \frac{\partial f(x^k)}{\partial x}^{-1} f(x^k) \tag{3.13}$$

Where, k is the iteration number and x^k is the state vector at k^{th} iteration.

The equation (3.10) can be further simplified as,

$$G(x) = \frac{\partial f(x^k)}{\partial x} = H^T(x^k)R^{-1}H(x^k) \tag{3.14}$$

The above equation result in a sparse, symmetric and positive definite matrix during the solution process and it is termed as gain matrix$G(x)$ [18].

Now, from (3.10), (3.11) and (3.12) the iterative solution structure can be rearranged as shown in equation below.

$$x^{k+1} = x^k + \left(H^T(x^k)\, R^{-1}\, H(x^k)\right)^{-1}.H^T.(x^k)\, R^{-1}\, (Z - h(x^k)) \qquad (3.15)$$

Convergence of (14) is satisfied when,

$$\max(x^{k+1} - x^k) \leq \epsilon \qquad (3.16)$$

Where, ϵ is a predetermined convergence factor

The errors are calculated as,

$$e_i = Z_{i\,measured} - h_i(x) \qquad (3.17)$$

This concludes the weighted lease square (WLS) approach for state estimation of a power system. The next section describes about implementation of WLS method on a distribution network.

3.4 State estimation formulation for a three phase power distribution network

The traditional power flow equations but modeled for a three phase power distribution network are used in this research. In this model, there are six state variables at each bus i.e. voltage magnitudes V_i^a, V_i^b, V_i^b and phase angles $\theta_i^a, \theta_i^b, \theta_i^c$.

In today's automated power distribution system the measurement of power injection at buses, power flow in the lines, bus voltages and line currents is possible. Hence, the system can be assumed to have abundant measurement data which in turn makes the system observable.

3.4.1 Measurement Data

The measurement data used in this research are as follows:

- V_{abc} Three phase voltage magnitudes at all buses
- P_i Real power injection at bus 'i' (scheduled or measured)
- Q_i Reactive power injection at bus 'i' (scheduled or measured)
- P_{ij} Real power flow from bus 'i' to bus 'j'
- Q_{ij} Reactive power flow from bus 'i' to bus 'j'
- I_{ij} Current flow from bus 'i' to bus 'j'

As shown in the diagram below, the symbols on the three-phase line 'ij' represents the measurement device.

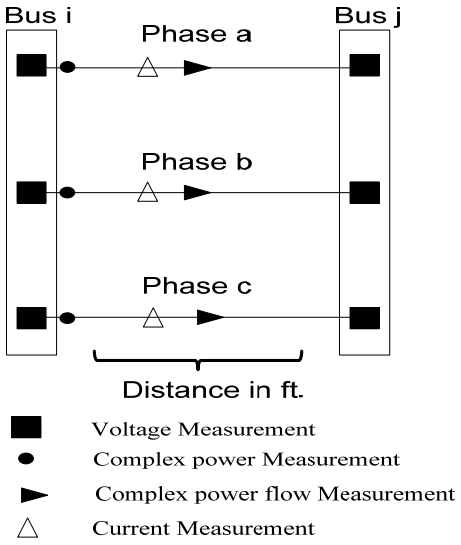

Figure 3.1 Three-phase measurement unit symbols

The mathematical model which relates the measurement values to its corresponding equations is explained in the next section.

3.4.2 Mathematical model

All the measurement equations used for the state estimation is represented in the form of Equation (3.2).

a. Three phase voltage equations at bus 'i' is given as

$$\text{a.} \quad \widehat{V_i^a} = V_i^a + e_{vi}^a$$

$$\text{b.} \quad \widehat{V_i^a} = V_i^b + e_{vi}^b$$

$$\text{c.} \quad \widehat{V_i^c} = V_i^c + e_{vi}^c \tag{3.18}$$

b. Three phase real power and reactive power injection at bus 'i' is represented as,

$$\widehat{P_i^P} = V_i^P \sum_{j=1}^{n} \sum_{m=1}^{3} V_j^m \left[G_{ij}^{Pm} \cos\left(\theta_{ij}^{Pm}\right) + B_{ij}^{Pm} \sin\left(\theta_{ij}^{Pm}\right)\right] + e_{Pi}^P \tag{3.19}$$

$$\widehat{Q_i^P} = V_i^P \sum_{j=1}^{n} \sum_{m=1}^{3} V_j^m \left[G_{ij}^{Pm} \sin\left(\theta_{ij}^{Pm}\right) - B_{ij}^{Pm} \cos\left(\theta_{ij}^{Pm}\right)\right] + e_{Qi}^P \tag{3.20}$$

c. Three phase real and reactive power flow from bus 'i' to bus 'j' is given as,

$$\widehat{P_{ij}^P} = (V_i^P)^2 - V_i^P V_j^P \left(g_{ij}^P cos\theta_{ij}^P + b_{ij}^P sin\theta_{ij}^P\right) + e_{Pij}^p \tag{3.21}$$

$$\widehat{Q_{ij}^P} = -(V_i^P)^2 - V_i^P V_j^P \left(g_{ij}^P sin\theta_{ij}^P - b_{ij}^P cos\theta_{ij}^P\right) + e_{Qij}^p \tag{3.22}$$

d. Three phase current flow in the line 'ij' is represented as,

$$\widehat{I_{ij}^P} = \sqrt{\left[(g_{ij}^P)^2 + (b_{ij}^P)^2\right]\left[(V_i^P)^2 + (V_j^P)^2 - 2V_i^P V_j^P \cos(\theta_{ij}^P)\right]} + e_{Iij}^P \tag{3.23}$$

3.4.3 Observability Analysis based Measurement Selection Technique (OA-MST)

One of the primary assumptions is that, the measurement values are available in abundant due to improvements in automated distribution automation (ADA) systems, which implies that with sufficient or more than sufficient measurement vectors, the whole system is observable and it is possible to obtain all the state variables from the state estimation algorithm. This can be justified by calculating the rank of measurement

Jacobian matrix, and if the rank is equal to the number of unknown state variables then the system can be trusted to be fully observable [32] and [33].

As mentioned in section 3.1, it is not required to process all the data from all the measurement units available. So, the not-so-important measurement units are removed by the algorithm during state estimation procedure without compromising the observability.

A new technique has been introduced in the developed algorithm. This technique will first scan all the available measurement units and selects a set of predetermined measurement values based on the meter variance factor (V.F) and the measurement importance factor (I.F).

$$Selection\ criteria = I.F + \frac{1}{V.F} \tag{3.24}$$

The first scan will consider all the measurement units with low variance factor and high importance factor. This is achieved by using the selection criteria function as shown in Equation (3.24). All the measurements units with high value in the 'selection criteria' value are shortlisted in descending order and are checked for observability. If the system is observable, it continues to perform state estimation. If the system is unobservable then the algorithm goes back to measurement data center and adds another measurement unit to the existing set and the process continues till the system is observable. The flow chart of the developed techniques is shown in Figure 3.2.

3.4.4 Load Modeling Technique (LMT) for distribution system state estimation

Load modeling is very important in state estimation of distribution system in order to obtain precise values of state variables [2]. The different types of load models are explained clearly in chapter 2. Three types of common load models used in power

distribution system are constant impedance load (Z_{load}), constant current load (I_{load}), constant power load (P_{load}). These $(ZIP)_{load}$ models can be formulated for real power injection and reactive power injection at the load bus as shown in (3.25)-(3.28)

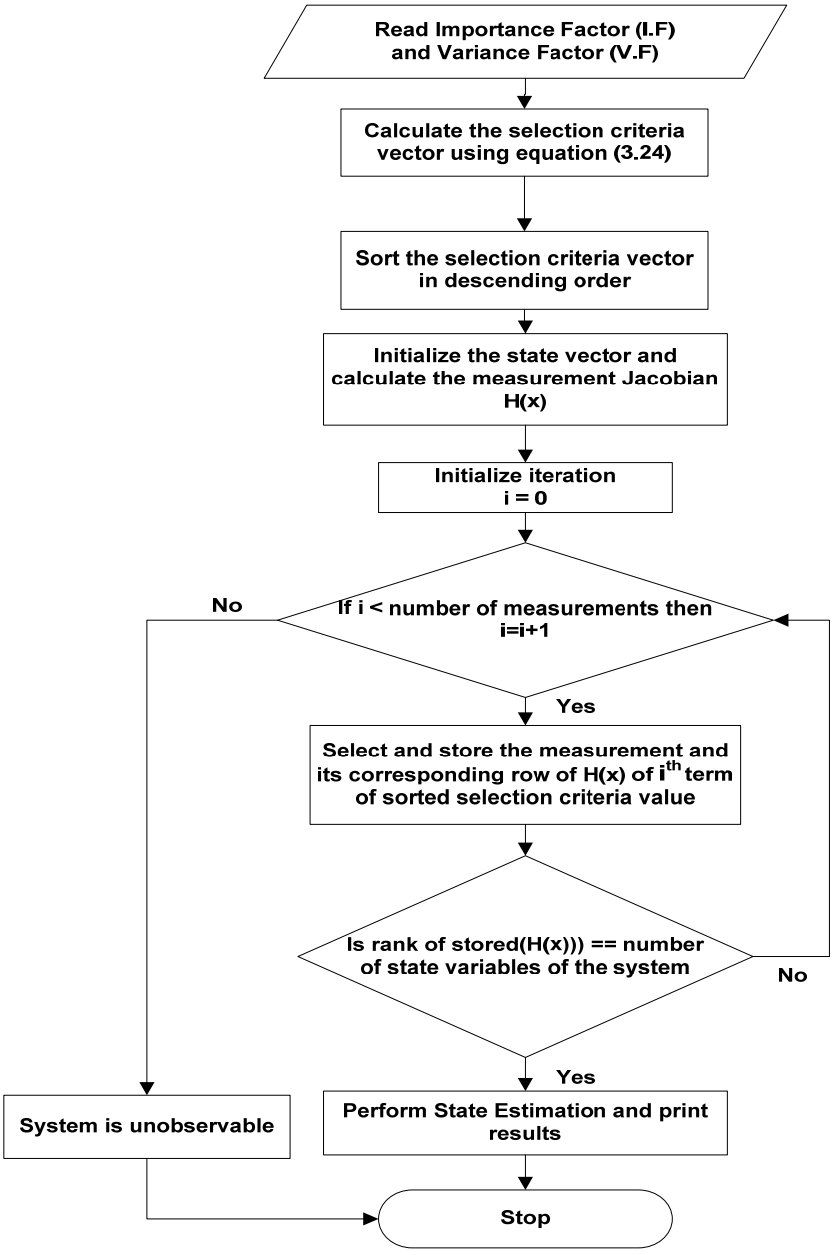

Figure 3.2 Flow chart for observability analysis

a. $$P_i^p{}_{Z_{load}} = \left|\widehat{S_i^p}\right| * \left(\left|V_i^2\right| \cos(Z_\theta)\right)$$

b. $$Q_i^p{}_{Z_{load}} = \left|\widehat{S_i^p}\right| * \left(\left|V_i^2\right| \sin(Z_\theta)\right) \quad (3.25)$$

a. $$P_i^p{}_{I_{load}} = \left|\widehat{S_i^p}\right| * \left(|V_i| \cos(I_\theta)\right)$$

b. $$Q_i^p{}_{I_{load}} = \left|\widehat{S_i^p}\right| * \left(|V_i| \sin(I_\theta)\right) \quad (3.26)$$

a. $$P_i^p{}_{P_{load}} = \left|\widehat{S_i^p}\right| * \left(\cos(P_\theta)\right)$$

b. $$Q_i^p{}_{P_{load}} = \left|\widehat{S_i^p}\right| * \left(\sin(P_\theta)\right) \quad (3.27)$$

Where,Z_θ,I_θ and P_θ are the impedance angle, current angle and the power angle respectively.

If any particular bus/node in a distribution system contains a load model which has a combination of all the three load types, then the equations for real and reactive power are given as,

a. $$P_i^p{}_{mixed_{load}} = \%\, P_i^p{}_{Z_{load}} + \%\, P_i^p{}_{I_{load}} + \%\, P_i^p{}_{P_{load}}$$

b. $$Q_i^p{}_{mixed_{load}} = \%\, Q_i^p{}_{Z_{load}} + \%\, Q_i^p{}_{I_{load}} + \%\, Q_i^p{}_{P_{load}} \quad (3.28)$$

3.4.5 Algorithm development

The iterative solution for the developed state estimation algorithm including observability, load modeling and WLS method is outlined as:

1. Start iteration count (k) and set ‘k’ = 0.
2. Initialize the state variable at a flat start.
3. Perform the observability analysis as explained in the flow chart I
4. Model all the loads using equations (24) - (27)

5. Calculate the corresponding non - linear vector, i.e. $h(x^k)$ using equations from (3.18) – (3.23)
6. Solve the measurement Jacobian matrix $J = H(x^k) = \left[\frac{\partial h(x^k)}{\partial x}\right]$
7. Form the error co-variance matrix as shown in equation (3.8)
8. Calculate the gain matrix $G(x^k) = \left(H^T(x^k)R^{-1}H(x^k)\right)$
9. Calculate $H^T(x^k)R^{-1}(Z - h(x^k))$
10. Solve $\Delta x = x^{k+1} - x^k = \left(G(x^k)\right)^{-1} H^T(x^k)R^{-1}(Z - h(x^k))$
11. Test for convergence, ($Max(x^{k+1} - x^k) \leq \epsilon$.
12. If no, update $x^{k+1} = x^k + \Delta x, k = k + 1$, and go-to step # 5. Else, go-to step 13.
13. Calculate the residuals and print state variables
14. Stop

Thus, the static state estimation solution for an unbalanced three phase radial distribution system can be achieved.

CHAPTER IV

RESULTS AND DISCUSSION

4.1 Load flow results

The developed load flow algorithm for an unbalanced radial type distribution system has been implemented for IEEE 4-bus feeder , 13-bus feeder and 37-bus feeder and the effectiveness of the method developed is explained in this section [25].

4.1.1 IEEE – 4 bus system

The IEEE-4 bus test feeder is taken as a base case for explaining the developed load flow algorithm in detail. For understanding of our comprehensive load flow algorithm, let us modify the 4-bus test feeder by adding a voltage regulator at bus - 4, a capacitor bank is also place at bus-4 and a switch is located between bus-1 and bus-2.

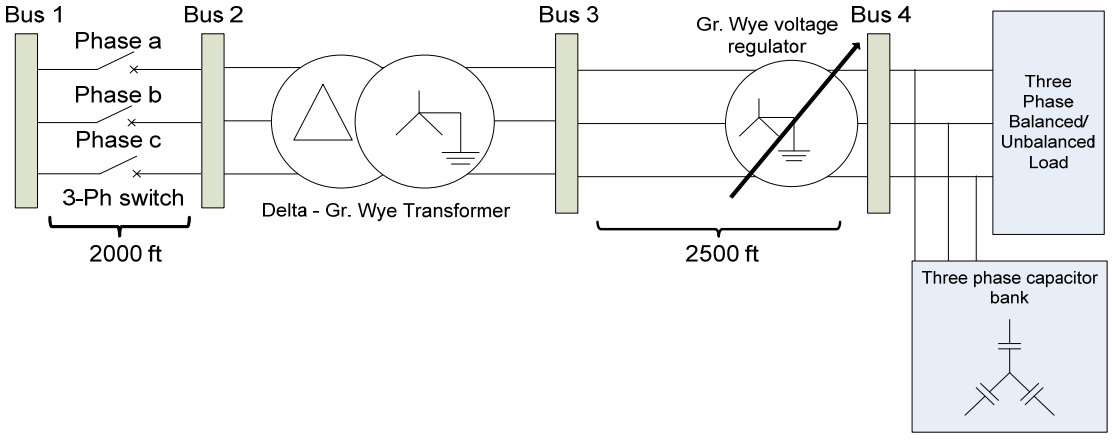

Figure 4.1 IEEE - 4 bus test system

A three phase transformer is place between bus-2 and bus-3. The modified IEEE-4 bus is shown in figure 4.1.

The below tables contain the line data, load data and network components data. It is taken from the IEEE – 4 bus document [26].

Table 4.1 Three phase load data of IEEE – 4 bus feeder

Bus-4	Phase	Balanced	Unbalanced
Load	A	1800 / 0.9 lag	1275 / 0.85 lag
Load	B	1800 / 0.9 lag	1800 / 0.9 lag
Load	C	1800 / 0.9 lag	2375 / 0.95 lag

The load can be connected in either wye or delta fashion.

Table 4.2 Three phase Transformer data of IEEE – 4 bus feeder

Connection type	kVA	kVLL-Primary	kVLL-Secondary	%R	%X
Step-Down	6,000	12.4	4.1	1.0	6.0

It is assumed that all the four types of transformers have the same rating as given above.

Table 4.3 Capacitor Data of IEEE – 4 bus system

Bus #	Phase - A	Phase – B	Phase - C
	kVAr	kVAr	kVAr
4	200	200	200

The capacitor bank is connected in wye fashion for this case.

Table 4.4 Regulator Data of IEEE – 4 bus feeder

Location	Bus - 4
Bandwidth	2.0 volts
Potential Transformer (PT) Ratio	20
Primary Current Transformer (CT) ratio	600
Phase monitored	A-B-C
Voltage Level	120 V

Connection type of this voltage regulator is grounded wye type and the taps function independently of each other.

The impedance matrix for a four wire configuration is given as,

$$Z_{1-2}^{abc} = \begin{bmatrix} 0.4576 + 1.078j & 0.1559 + 0.5017j & 0.1535 + 0.3849j \\ 0.1559 + 0.5017j & 0.4666 + 1.0482j & 0.158 + 0.4236j \\ 0.1535 + 0.3849j & 0.158 + 0.4236j & 0.4615 + 1.0651j \end{bmatrix} \Omega/mile$$

The impedance matrix for a three wire configuration is given as,

$$Z_{3-4}^{abc} = \begin{bmatrix} 0.4013 + 1.4133j & 0.0953 + 0.8515j & 0.0953 + 0.7266j \\ 0.0953 + 0.8515j & 0.4013 + 1.4133j & 0.0953 + 0.7802j \\ 0.0953 + 0.7266j & 0.0953 + 0.7802j & 0.4013 + 1.4133j \end{bmatrix} \Omega/mile$$

The source is an infinite bus with 12.47 kV_{LL} and the switch at bus - 1 is in 'on' state.

Now, by considering all the above given network data and implementing the load flow algorithm in Matlab, we get the comprehensive load flow results as shown in the tables below.

The first set of results as given in table 4.5 are obtained by considering,

- Four different types of step-down transformers
- Three-phase wye - connected loads
- Three-phase delta - connected loads

The second set of results as given in table 4.6 are obtained by considering

- Three phase wye connected shunt capacitor at bus - 4
- Three phase wye connected voltage regulator at bus - 4
- Three phase delta- grounded wye transformer
- Balanced three phase wye-connected load

Table 4.5 Load flow results for an IEEE 4– bus with different types of transformers

Connection	Gr Y – Gr Y	D - D	D – Gr Y	Gr. Y - D
Bus 2	V.mag / Angle	V.mag / Angle	V.mag / Angle	V.mag / Angle
V_a	7106.0/-0.3515	12317/29.714	12340/29.73	7123.1/-0.3372
V_b	7141.4/-120.34	12351/-90.36	12349/-90.40	7142/-120.38
V_c	7119.7/119.63	12341/149.592	12318/149.62	7137.6/119.569
Bus 3				
V_a	2247.2/-3.707	3903/26.4	2249/-33.64	4060.4/-1.3923
V_b	2269.1/-123.471	3915/-93.59	2266/-153.49	4071.1/-121.428
V_c	2255.4/116.403	3912/146.36	2257/86.3537	4069.2/118.522
Bus 4				
V_a	1917/-9.09	3435/22.3	1919/-38.99	3733.9/-1.4920
V_b	2062.1/-128.31	3497/-99.31	2058/-158.34	3800.3/-122.2147
V_c	1980.2/110.86	3391/140.633	1983/80.82	3764.0/117.598
Current 1-2				
I_a	348/-34.93	335.8/-34.62	334.9/-35.68	309.5/-27.33
I_b	323.6/-154.15	336/-154.66	331.8/-154.0	304.08/-148.05
I_c	336.6/85.02	335.7/85.33	341.8/85.6097	303.47/93.19
Current 3-4				
I_a	1043.1/-34.93	1006.7/-34.62	1042.1/-64.84	919.78/-57.65
I_b	9699/-154.14	1007.3/-154.66	971.9/175.813	922.9/-177.98
I_c	1010/85.02	1006.4/85.33	1008.7/54.978	916.8/62
Load	1800+j871.8	1800+j871.8	1800+j871.8	1815+j0.876
Iteration	16	13	15	8
Tolerance	0.0001	0.0001	0.0001	0.001

A standard 30 degree phase shift is assumed for wye-delta and delta-wye connection. The voltages for grounded-wye connection are phase - neutral voltage and the voltages for delta connections are phase - phase voltage. The currents are line-currents.

From the results, we can see that the power factor is improved when the effect of shunt capacitors was considered and we can also see a significant improvement in the voltage profile when a three phase voltage regulator was used at bus – 4.

These results justify our comprehensive load flow algorithm.

Table 4.6 Comprehensive load flow results for an IEEE 4– bus feeder

Connection	Only D – Gr. Wye	D – Gr. Wye with Shunt Capacitor	D – Gr. Wye with Voltage Regulator		
Bus 2	Voltage/angle	Voltage/Angle	Voltage/angle		
V1	12340/29.73	12355/29.73	12344/29.73		
V2	12349/-90.40	12365/-90.42	12355/-90.40		
V3	12318/149.62	12336/149.59	12326/149.62		
Bus 3					
V1	2249/-33.64	2271/-33.64	2258/-33.64		
V2	2266/-153.49	2288/-153.52	2270/-153.49		
V3	2257/86.3537	2281/86.33	2265/86.3537		
Bus 4					
V1	1919/-38.99	1976/-39.271	2410/-37.619		
V2	2058/-158.34	2113/-158.55	2406/-157.56		
V3	1983/80.82	2046/80.72	2469/81.99		
Current 1-2					
Ia	334.9/-35.68	311.49/-30.566	276.94/-33.39		
Ib	331.8/-154.0	309.5/-148.5939	274.4/-154.05		
Ic	341.8/85.6097	319.72/90.7249	272.9/86.739		
Current 3-4					
Ia	1042.1/-64.84	974.40/-60.07	829.46/-63.46		
Ib	971.9/175.813	906.76/178.6	831.34/176.59		
Ic	1008.7/54.978	938.62/60.30	810.06/56.15		
Power factor	0.900	0.9348	0.900		
Iteration	15	16	13		
Tolerance	0.0001	0.0001	0.0001		
Tap position	--	--	Ph-a	Ph-b	Ph-c
			27	21	27

A standard 30 degree phase shift is assumed for delta-wye connection. The voltages for grounded-wye connection are phase - neutral voltage and the voltages for delta connections are phase - phase voltage. The currents are line-currents.

The developed algorithm is also tested on two other cases and the results are presented in the next section.

4.1.2 IEEE – 13 bus system

The IEEE- 13 bus distribution feeder [27] is as shown in figure 4.2.

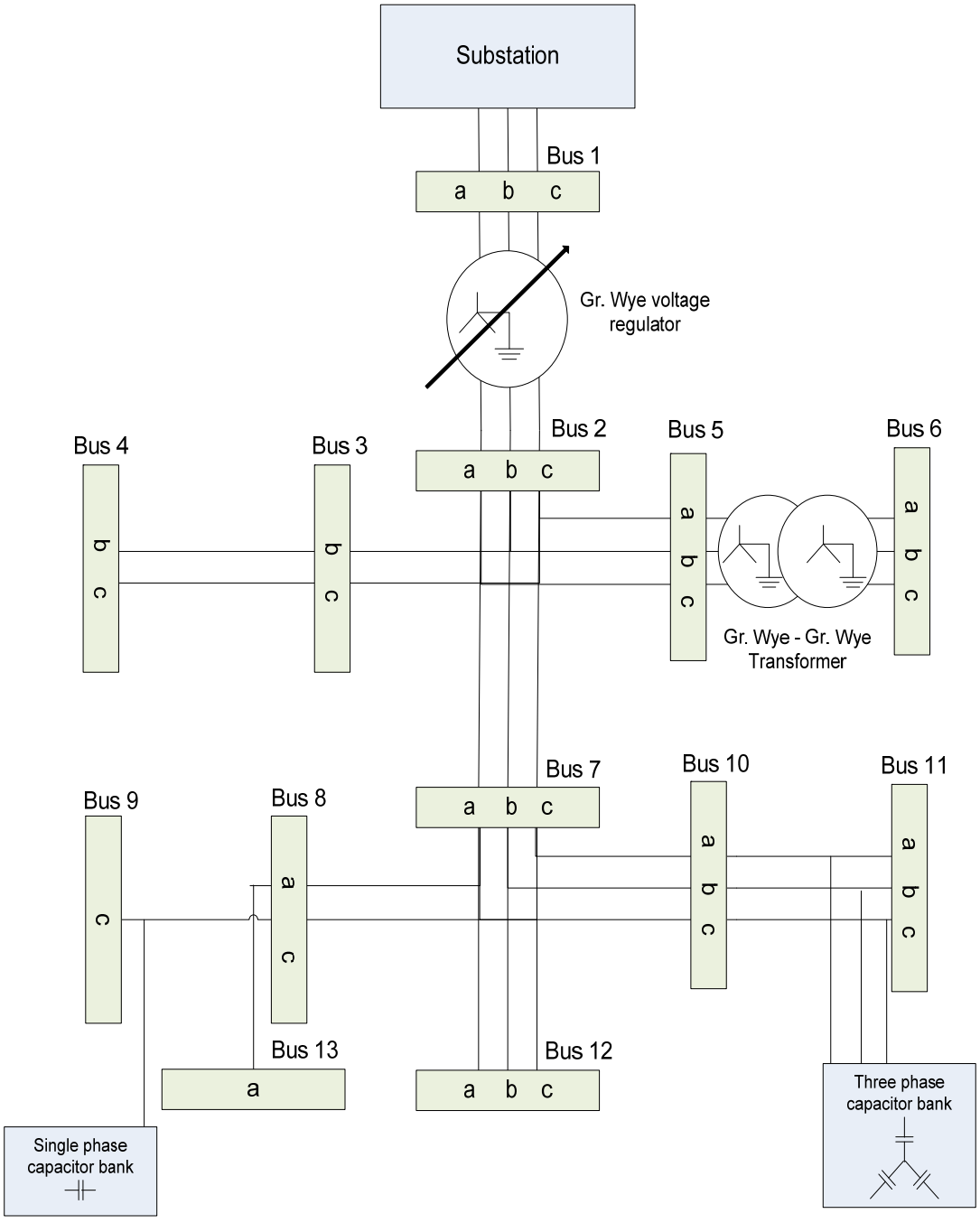

Figure 4.2 IEEE - 13 bus test system

The load flow algorithm converged after 4 iterations with a tolerance of 0.001. The results are shown in table below.

Table 4.7 Comprehensive load flow results for an IEEE 13– bus feeder

Bus #	V-mag. (p.u)	V-Angle	V-mag. (p.u)	V-Angle	V-mag. (p.u)	Angle
	A-N		B-N		C-N	
1	1.00	0	1.00	-120	1.00	120
2	0.9756	-1.2652	0.9707	-121.282	0.9621	118.4661
3	--	--	0.9657	-121.352	0.9596	118.4271
4	--	--	0.9641	-121.383	0.9580	118.4073
5	0.9742	-1.300	0.9696	-121.308	0.9610	118.4383
6	0.9701	-1.421	0.9664	-121.396	0.9577	118.3518
7	0.9557	-2.414	0.9548	-122.008	0.9364	117.2479
8	0.9547	-2.425	--	--	0.9352	117.2232
9	--	--	--	--	0.9340	117.1984
10	0.9523	-2.5621	0.9523	-122.052	0.9318	117.1447
11	0.9496	-2.5866	0.9518	-122.039	0.9299	117.1570
12	0.9557	-2.4136	0.9548	-122.009	0.9364	117.2479
13	0.9527	-2.3951	--	--	--	--

4.1.3 IEEE – 37 bus system

The IEEE – 37 bus test feeder developed by the IEEE distribution committee [28] is as shown in the figure below.

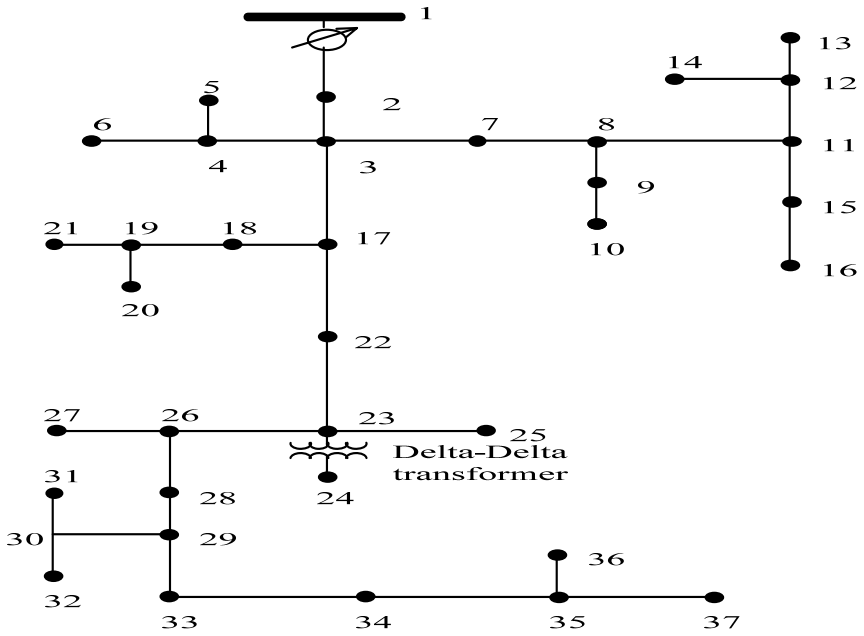

Figure 4.3 IEEE -37 bus test system

The above distribution system is delta type underground cable network [28].

Table 4.8 Comprehensive load flow results for an IEEE 37– bus feeder

Bus #	V-mag. (p.u)	V-Angle	V-mag. (p.u)	V-Angle	V-mag. (p.u)	Angle
	A-N		B-N		C-N	
1	1.00	30	1.00	-90	1.00	150
2	0.9804	29.885	0.9858	-90.0640	0.9675	149.799
3	0.9775	29.868	0.9839	-90.0730	0.9634	149.772
4	0.9775	29.867	0.9838	-90.0728	0.9620	149.770
5	0.9775	29.867	0.9838	-90.0725	0.9616	149.781
6	0.9775	29.867	0.9838	-90.0721	0.9615	149.782
7	0.9771	29.8664	0.9827	-90.0724	0.9625	149.770
8	0.9764	29.8649	0.9810	-90.0714	0.9617	149.768
9	0.9762	29.8657	0.9810	-90.0712	0.9617	149.768
10	0.9753	29.8700	0.9810	-90.0712	0.9617	149.768
11	0.9764	29.8649	0.9786	-90.0699	0.9606	149.765
12	0.9764	29.8648	0.9753	-90.0448	0.9602	149.767
13	0.9764	29.8648	0.9746	-90.0401	0.9602	149.768
14	0.9764	29.8649	0.9749	-90.0422	0.9601	149.768
15	0.9764	29.8649	0.9783	-90.0697	0.9606	149.765
16	0.9763	29.8649	0.9781	-90.0678	0.9606	149.765
17	0.9743	29.8481	0.9828	-90.0783	0.9602	149.751
18	0.9736	29.8521	0.9826	-90.0767	0.9598	149.754
19	0.9732	29.8517	0.9825	-90.0766	0.9596	149.754
20	0.9730	29.8528	0.9823	-90.0753	0.9594	149.755
21	0.9729	29.8532	0.9825	-90.0766	0.9596	149.754
22	0.9714	29.8442	0.9819	-90.0785	0.9571	149.746
23	0.9705	29.8430	0.9815	-90.0786	0.9563	149.744
24	0.9705	29.8430	0.9815	-90.0786	0.9563	149.744
25	0.9705	29.8430	0.9809	-90.0791	0.9563	149.744
26	0.9690	29.8409	0.9814	-90.0785	0.9550	149.742
27	0.9690	29.8409	0.9814	-90.0785	0.9547	149.744
28	0.9674	29.8388	0.9812	-90.0784	0.9538	149.740
29	0.9654	29.8367	0.9809	-90.0782	0.9519	149.736
30	0.9654	29.8367	0.9804	-90.0750	0.9509	149.741
31	0.9654	29.8367	0.9794	-90.0670	0.9509	149.741
32	0.9654	29.8367	0.9804	-90.0750	0.9506	149.743
33	0.9631	29.8342	0.9809	-90.0782	0.9507	149.734
34	0.9642	29.8333	0.9809	-90.0782	0.9500	149.732
35	0.9624	29.8330	0.9809	-90.0782	0.9493	149.731
36	0.9624	29.8330	0.9809	-90.0782	0.9490	149.733
37	0.9624	29.8330	0.9809	-90.0782	0.9491	149.731

Table 4.9 Observations

Items	IEEE -4	IEEE-13	IEEE-37
Total number of iterations	4	4	4
Time for computation (sec) (MATLAB 10a and i5 processor)	0.001	0.005	0.02
Tolerance value for convergence	0.01	0.01	0.01

As seen from the above table, we can conclude that the time taken by the comprehensive load flow algorithm is very less and increases gradually as the system size increases. Also, the number of iterations is found to be constant for the same tolerance value for all the three IEEE distribution test feeders.

4.2 State estimation results

The state estimation (SE) algorithm is solved for a radial type unbalanced three phase power distribution network using the equations developed in chapter 3 and by applying the weighted least square method. The results obtained are presented in the next sections 4.2.1 - 4.2.3. The SE algorithm is implemented on IEEE 4-bus system, 13-bus system and 37-bus system.

4.2.1 IEEE – 4 bus system

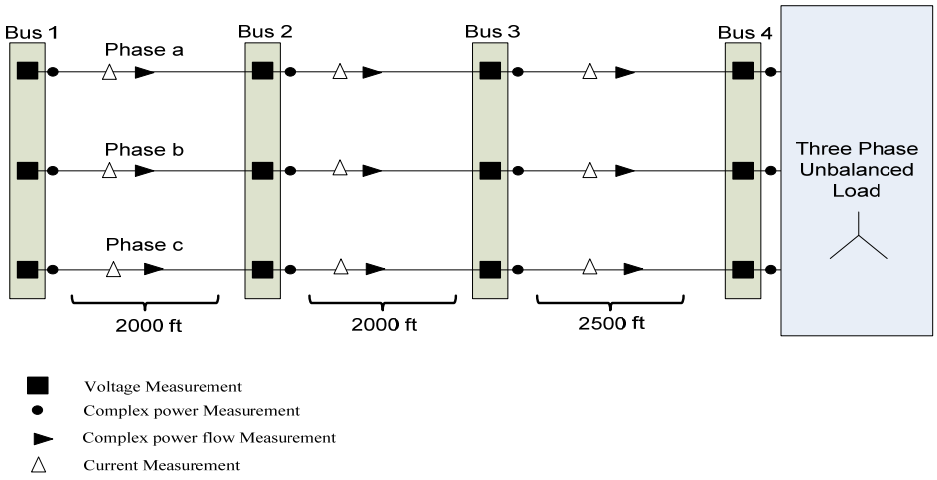

Figure 4.4 Modified IEEE 4-bus system with measurement units.

A modified IEEE-4 bus radial type test system as shown in figure 4.3 is considered as the base case to explain our developed state estimation algorithm.

The line parameters, load types and load values for this system are given in the above section 4.1.1. This 4-bus distribution system has twenty four (24) state variables and forty five (45) measurement units.

The results from power flow solution obtained in chapter 3 are used as measurement data. All the measurement data is represented in per unit format along with the meter importance factor (M.I.F) and meter variance factor (M.V.F). The M.I.F value is selected based on experience and literature review; whereas the measurement M.V.F is taken from the state estimation book by Abur, Ali [13].

Table 4.10 Voltage Measurement Data for 4 – bus feeder

Bus #	V-mag.(p.u)	V-mag.(p.u)	V-mag.(p.u)	I.F	V.F
	Ph.- A	Ph.- B	Ph.- C		
1	1	1 1		10	0.004
2	0.9723	0.9724	0.9721	10	0.004
3	0.9683	0.9684	0.9681	10	0.004
4	0.9382	0.9382	0.9381	10	0.004

Table 4.11 Power Flow Measurement Data for 4 – bus feeder

From-Bus	To-Bus	Ph.- A		Ph.- B		Ph.- C		I.F		V.F	
		P_{flow} (kW)	Q_{flow} (kVAr)	P_{flow} (kW)	Q_{flow} (kVAr)	P_{flow} (kW)	Q_{flow} (kVAr)	P_{flow}	Q_{flow}	P_{flow}	Q_{flow}
1	2	1860	1040	1860	1040	1860	1040	9	8	0.008	0.008
2	3	1840	960	1840	960	1830	960	9	8	0.008	0.008
3	4	1830	950	1830	950	1830	950	9	8	0.008	0.008

Table 4.12 Injected Power Measurement Data for 4 – bus feeder

Bus #	Ph.- A		Ph.- B		Ph.- C		I.F		V.F	
	P_{inj} (kW)	Q_{inj} (kVAr)	P_{inj} (kW)	Q_{inj} (kVAr)	P_{inj} (kW)	Q_{inj} (kVAr)	P_{inj}	Q_{inj}	P_{inj}	Q_{inj}
4	1800	870	1800	870	1800	870	7	6	0.01	0.01

Table 4.13 Current Flow Measurement Data for 4 – bus feeder

From-Bus	To-Bus	Ph.-A	Ph.-B	Ph.- C	I.F	V.F
		I_{flow}(kA)	I_{flow}(kA)	I_{flow}(kA)		
1	2	21.3	21.4	21.2	5	0.01
2	3	21.3	21.4	21.2	5	0.01
3	4	21.3	21.4	21.2	5	0.01

All the calculations for state estimation have been done by transforming all the parameters in to wye - connection for easy of understanding and calculation. The effective impedance of the transformer is considered as line impedance between bus 2 and bus 3. Table 4.10 - Table 4.13 shows the measurement values for the 4 bus test feeder.

The developed state estimation algorithm is coded in MATLAB by considering all the given measurement data. The solution steps can be illustrated as,

- The code scans all the I.F and V.F data and generates the 'selection criteria' vector according to equation 3.24.
- Then it initializes the state variable at a flat start and calculates the measurement initial Jacobian matrix. This is used to check the condition of observability.
- Based on 'selection criteria vector' the code checks for observability conditions as explained in the section 3.4.3
- The selected measurement for the above problem is given in table 4.14
- Then the code performs the state estimation based on WLS method using the equation modeled for three-phase networks.
- The state variable obtained as the solution is given in table 4.12

As shown in table 4.14, the algorithm selected only twenty one (21) measurements units out of total forty five (45) units. Only these twenty one measurements are used to perform state estimation. This reduces the computation time and system memory significantly on large distribution networks.

Table 4.14 Selection Criteria Vector

Measurement	Selection criteria value	Rank of $H(x)$
V_1^a	260	1
V_1^b	260	2
V_1^c	260	3
V_2^a	260	4
V_2^b	260	5
V_2^c	260	6
V_3^a	260	7
V_3^b	260	8
V_3^c	260	9
V_4^a	260	10
V_4^b	260	11
V_4^b	260	12
$P_{flow1-2}^a$	134	13
$P_{flow1-2}^b$	134	14
$P_{flow1-2}^c$	134	15
$P_{flow2-3}^a$	134	16
$P_{flow2-3}^b$	134	17
$P_{flow2-3}^c$	134	18
$P_{flow3-4}^a$	134	19
$P_{flow3-4}^b$	134	20
$P_{flow3-4}^c$	134	21

Where, V_1^a is voltage measurement of bus – 1, phase – a.

Table 4.15 State Variables obtained for a 4 – bus feeder

Bus #	V-mag. (p.u)	V-Angle	V-mag. (p.u)	V-Angle	V-mag. (p.u)	Angle
	A-N		B-N		C-N	
1	1.000	0	1	-120.00	1	120.00
2	0.972	-1.648	0.973	-121.64	0.972	118.35
3	0.968	-1.965	0.968	-122.00	0.967	118.00
4	0.938	-3.4997	0.937	-123.43	0.938	116.52

The voltages are in per unit (p.u) and angles in degree

The obtained state variables from the developed state estimation algorithm are given in the table 4.15. The state estimation solution of IEEE 4-bus test feeder converged after 4 iterations with a tolerance of 0.001.

Table 4.16 Observations

Total # of available measurements units	45
Total # of measurement units selected by the developed algorithm	21
Time for computation (MATLAB 10a and i5 processor) : Normal method	0.27 sec
Time for computation (MATLAB 10a and i5 processor) : Developed method	0.21 sec

From the above table we can see that the computational time has improved.

4.2.2 IEEE – 13 bus system

The modified IEEE-13 bus radial type distribution network is as shown in Figure 4.4. A total of 157 measurements values were given as inputs to the algorithm, where only 61 measurements were selected for performing state estimation. The measurement values are obtained from the load flow result and all the system parameters are considered in per-unit values.

Table 4.17 State Variables obtained for a 13 – bus feeder with only CP loads

Bus #	V-mag. (p.u)	V-Angle	V-mag. (p.u)	V-Angle	V-mag. (p.u)	V-Angle
	A-N		B-N		C-N	
1	1.00	0	1.00	-120	1.00	120
2	0.9756	-1.2652	0.9707	-121.282	0.9621	118.4661
3	--	--	0.9657	-121.352	0.9596	118.4271
4	--	--	0.9641	-121.383	0.9580	118.4073
5	0.9742	-1.300	0.9696	-121.308	0.9610	118.4383
6	0.9701	-1.421	0.9664	-121.396	0.9577	118.3518
7	0.9557	-2.414	0.9548	-122.008	0.9364	117.2479
8	0.9547	-2.425	--	--	0.9352	117.2232
9	--	--	--	--	0.9340	117.1984
10	0.9523	-2.5621	0.9523	-122.052	0.9318	117.1447
11	0.9496	-2.5866	0.9518	-122.039	0.9299	117.1570
12	0.9557	-2.4136	0.9548	-122.009	0.9364	117.2479
13	0.9527	-2.3951	--	--	--	--

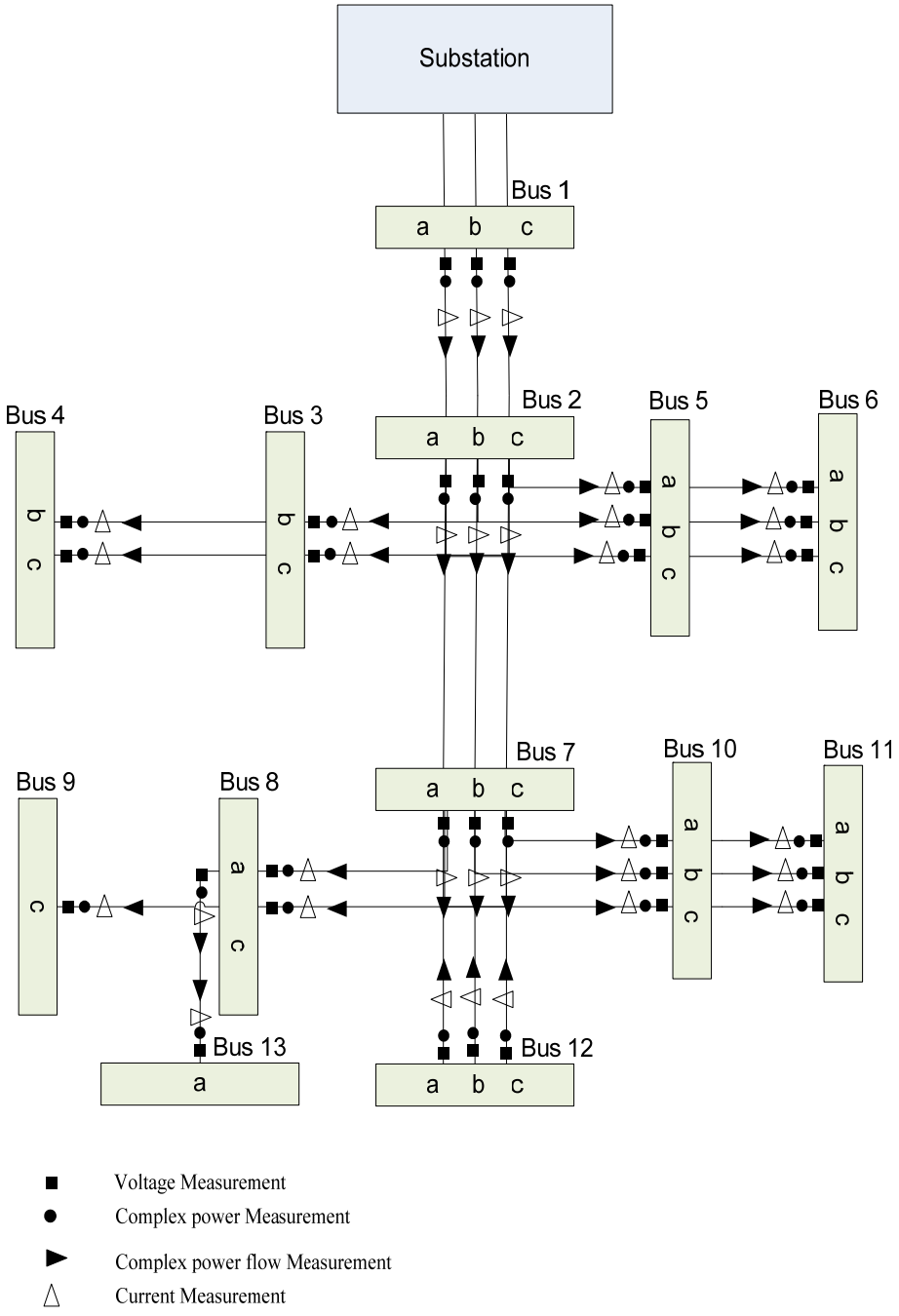

Figure 4.5 Modified IEEE-13 bus test system with measurement units

State estimation algorithm is solved for two cases for this test feeder. In first case, it is assumed that all the loads are constant power (CP) type loads and in second case the loads models consisted of all the three types as explained in chapter 2.

Table 4.17 shows the state variables obtained for only constant power type loads.

Table 4.18 shows the state variables obtained when all the three types of load models were considered for a 13 - bus test feeder.

Table 4.18 State Variables obtained for a 13 – bus feeder with only CP, CZ & CI loads

Bus #	V-mag. (p.u)	V-Angle	V-mag. (p.u)	V-Angle	V-mag. (p.u)	V-Angle
	A-N		B-N		C-N	
1	1.00	0	1.00	-120	1.00	120
2	0.9759	-1.2539	0.9713	-121.257	0.9634	118.5074
3	--	--	0.9665	-121.323	0.9610	118.4738
4	--	--	0.9650	-121.350	0.9596	118.4532
5	0.9745	-1.2889	0.9702	-121.283	0.9622	118.4809
6	0.9740	-1.4094	0.9670	-121.369	0.9590	118.3933
7	0.9563	-2.3882	0.9556	-121.973	0.9382	117.3193
8	0.9554	-2.3992	--	--	0.9371	117.2950
9	--	--	--	--	0.9360	117.2706
10	0.9529	-2.5364	0.9532	-122.015	0.9337	117.2198
11	0.9502	-2.5608	0.9528	-122.013	0.9318	117.2325
12	0.9563	-2.3882	0.9556	-121.973	0.9382	117.3193
13	0.9590	-2.3746	--	--	--	--

The state estimation algorithm converged after 4 iterations for both the cases.

4.2.3 IEEE – 37 bus system

The IEEE -37 bus feeder is shown in figure 4.3. Measurements values are available for all the branch flows and bus injections at all the buses. This implies that there are a total of 499 measurements available. The developed state estimation algorithm selected only 219 measurement units based on the selection criteria value.

The state estimation algorithm converged after 5 iterations with a tolerance of 0.001.

The state variables obtained is given in table 4.19.

Table 4.19 State Variables obtained for a 37-bus test feeder

Bus #	V-mag. (p.u)	V-Angle	V-mag. (p.u)	V-Angle	V-mag. (p.u)	V-Angle
	A-N		B-N		C-N	
1	1.0000	30	1.0000	-90	1.0000	150
2	0.9804	29.8848	0.9858	-90.0618	0.9675	149.8028
3	0.9775	29.8711	0.9839	-90.0732	0.9634	149.7732
4	0.9775	29.8711	0.9838	-90.0667	0.9620	149.7840
5	0.9775	29.8711	0.9838	-90.0667	0.9616	149.7816
6	0.9775	29.8711	0.9838	-90.0748	0.9615	149.7821
7	0.9771	29.8614	0.9827	-90.0692	0.9625	149.7662
8	0.9764	29.8613	0.9810	-90.0674	0.9617	149.7698
9	0.9762	29.8682	0.9810	-90.0729	0.9617	149.7698
10	0.9753	29.8771	0.9810	-90.0729	0.9617	149.7698
11	0.9764	29.8613	0.9786	-90.0639	0.9606	149.7603
12	0.9764	29.8613	0.9753	-90.0536	0.9602	149.7637
13	0.9764	29.8613	0.9746	-90.0377	0.9602	149.7637
14	0.9764	29.8613	0.9749	-90.0414	0.9601	149.7719
15	0.9764	29.8613	0.9783	-90.0688	0.9606	149.7603
16	0.9763	29.8613	0.9781	-90.0744	0.9606	149.7603
17	0.9743	29.8454	0.9828	-90.0737	0.9602	149.7514
18	0.9736	29.8608	0.9826	-90.0736	0.9598	149.7496
19	0.9732	29.8512	0.9825	-90.0806	0.9596	149.7535
20	0.9730	29.8561	0.9823	-90.0750	0.9594	149.7582
21	0.9729	29.8622	0.9825	-90.0806	0.9596	149.7535
22	0.9714	29.8474	0.9819	-90.0843	0.9571	149.7443
23	0.9705	29.8405	0.9815	-90.0759	0.9563	149.7403
24	0.9705	29.8405	0.9815	-90.0759	0.9563	149.7403
25	0.9705	29.8405	0.9809	-90.0833	0.9563	149.7403
26	0.9690	29.8363	0.9814	-90.0848	0.9550	149.7363
27	0.9690	29.8363	0.9814	-90.0848	0.9547	149.7402
28	0.9674	29.8434	0.9812	-90.0817	0.9538	149.7426
29	0.9654	29.8380	0.9809	-90.0823	0.9519	149.7306
30	0.9654	29.8380	0.9804	-90.0684	0.9509	149.7451
31	0.9654	29.8380	0.9794	-90.0724	0.9509	149.7451
32	0.9654	29.8380	0.9804	-90.0684	0.9506	149.7370
33	0.9631	29.8334	0.9809	-90.0823	0.9507	149.7380
34	0.9642	29.8326	0.9809	-90.0823	0.9500	149.7368
35	0.9624	29.8329	0.9809	-90.0823	0.9493	149.7356
36	0.9624	29.8326	0.9809	-90.0823	0.9490	149.7273
37	0.9624	29.8326	0.9809	-90.0823	0.9491	149.7324

CHAPTER V

CONCLUSION AND FUTURE WORK

5.1 Conclusion

In this thesis, an effective and comprehensive load flow tool is developed for a three phase unbalanced radial distribution network. Also developed in this thesis are, three different matrices viz. voltage adjustment matrix, current adjustment matrix and impedance adjustment matrix, which can incorporate all the distribution system components. These three matrices along with BIBC and BCBV are used extensively to solve the load flow problem. The proposed algorithm can be directly implemented on any balanced/unbalanced single/double/three-phase radial distribution system even with large number of buses. The proposed method has shown good convergence characteristics even for systems with high R/X value and for loads with high degree of unbalance.

A detailed description of the developed load flow method and its implementation has been discussed. This load flow algorithm is tested on IEEE-4 bus, IEEE -13 bus and IEEE-37 bus test feeders and the results were justified.

An efficient and computationally effective state estimation tool is developed for a radial type unbalanced three phase power distribution system. It has been observed that the accuracy of the estimated state variables have improved by using the load modelling technique (LMT) which is developed in this research. In-addition, the measurement selection technique based on observability analysis (OA-MST) helped to reduce the

computational time. Hence, by using these two developed techniques a fast and accurate solution is achievable.

A detailed description of WLS method and its implementation is discussed in this thesis. The state estimation algorithm is tested on IEEE 4, 13 and 37 bus test feeders and the results were found to be accurate. This developed tool can be incorporated with the existing power distribution system for online monitoring.

5.2 Future work

In any research, there is always a scope for improvements. The developed load flow algorithm is designed typically for a radial distribution system. As the time progresses, the algorithm can be modified such that, it can be applied to all types of distribution network as explained in chapter 1. This developed algorithm does not include the effects of distributed generation (DG) or renewable energy such as solar and wind energy systems, advanced research can be done in developing a robust load-flow algorithm which can incorporate the DG and renewable energy resources as well.

State estimation algorithm developed in this thesis is static in nature. There is a wide scope for implementing dynamic state estimation algorithm based on Kalman-filter technique in the near future for a power distribution network.

REFERENCES

[1] EATON manual on Power Distribution systems, 2013, EATON Corporation.

[2] Kersting, William H. Distribution System Modeling and Analysis, CRC Press, 2012.

[3] Yeleti, Sandeep, "Optimal operation of multi-terminal VSC based MVDC shipboard power system", Master thesis, Mississippi State University, 2010.

[4] Alsaadi, A., & Gholami, B. "An Effective Approach for Distribution System Power Flow Solution" Proc. WASET, Vol. 25, 2009, pp. 1 -23.

[5] Subrahmanyam, J. B. V. "Load Flow Solution of Unbalanced Radial Distribution Systems", Journal of Theoretical and Applied Information Technology, Vol. 6, No. 1, pp. 040-051.

[6] Das, D., Kothari, D.P., & Kalam, A. "Simple and efficient method for load flow solution of radial distribution networks" Butterworth – Heinemann, Electrical power & Energy Systems, Vol. 17, No. 5,1995, pp. 335-346.

[7] Prakash, K., & Sydulu, M. "An Effective Topological and Primitive Impedance based Three Phase Load Flow Method for Radial Distribution Systems" TENCON 2008 - 2008 IEEE Region 10 Conference, Vol. 1,2008, pp. 6.

[8] Stott, B., & Alsac, O. "Fast Decoupled Load Flow" IEEE Transactions on Power Apparatus and Systems, Vol. PSA-93, 1974, pp. 859-869.

[9] Chen, T.-H., Mo-Shing Chen, Hwang, K.-J., Kotas, P., & Chebli, E.A. "Distribution system power flow analysis- a rigid approach" IEEE Transactions on Power Delivery, Vol. 6, 1991, pp.1146-1152.

[10] Chang, G. W., Chu, S. Y., & Wang, H. L., "An Improved Backward/Forward Sweep Load Flow Algorithm for Radial Distribution Systems" IEEE Transactions on Power Systems, Vol. 22, 2007, pp. 882-884.

[11] Zhang, F., & Cheng, Carol S. "A Modified Newton Method for Radial Distribution System Power Flow Analysis" IEEE Transactions on Power Systems, Vol. 12, 1997, pp. 389-397.

[12] Toppo, Shilpa, “Development of current injection based three phase unbalanced continuation power flow for distribution system”, Master thesis, Mississippi State University, 2010.

[13] Abur, Ali, & Gomez-Exposito, Antonio, Power System State Estimation: Theory and Implementation, CRC Press, 2004.

[14] Lu, C.N., Teng, J. H., & W.-H.E. “Distribution system state estimation” IEEE Transactions on Power Systems, Vol. 10. No. 1, 1995, pp. 229-240.

[15] Hansen, C.W., & Debs, A.S. “Power system state estimation using three-phase models” IEEE Transactions on Power Systems, Vol. 10. No. 2, 1995, pp. 818-824.

[16] Ke Li, “State estimation for power distribution system and measurement impacts” IEEE Transactions on Power Systems, Vol. 11. No. 2, 1996, pp. 911-916.

[17] Youman Deng, Ying He, & Boming Zhang, “Branch-estimation-based state estimation for radial distribution systems” Power Engineering Society Winter Meeting, IEEE, Vol. 4, 2000, pp. 2351-2356.

[18] Schneider, K.P., Fuller, J.C., Chassin, D.P. “Multi-State Load Models for Distribution System Analysis” IEEE Transactions on Power Systems, Vol. 26. No. 4, 2011, pp. 2425-2433.

[19] Thukaram, D., Jerome Jovitha, & Surapong, C. “A robust three-phase state estimation algorithm for distribution networks” Elsevier, Electric Power Systems Research, 55, 2000, pp. 191 – 200.

[20] Karimi, M., Mokhlis, H., Bakar, A.H.A., Shahriari, A., Faradonbeh, M.A., & Rosli, H.M. “Impact of load modeling in distribution state estimation” Power Engineering and Optimization Conference (PEDCO), 2012, pp. 67 -71.

[21] Bhutad, A. G., Kulkarni, S.V., & Khaparde, S.A. “Three-phase load flow methods for radial distribution networks” TENCON 2003. Conference on Convergent Technologies for the Asia-Pacific Region, Vol. 2, 2003, pp. 781-785.

[22] Kersting, W.H., & Green, R.K. “The application of Carson’s equation to the steady-state analysis of distribution feeders” Power Systems Conference and Exposition (PSCE), 2011 IEEE/PES, 2011, pp. 1-6.

[23] Thukaram, D., Wijekoon Banda, H.M., & Jerome, Jovitha. “A robust three phase power flow algorithm for radial distribution systems” Elsevier, Electric Power Systems Research, 50, 1999, pp. 227 – 236.

[24] Khushalani, Sarika, “Development of power flow with distributed generators and reconfiguration for restoration of unbalanced distribution systems”, PhD dissertation, Mississippi State University, 2006.

[25] IEEE Distribution Planning Working Group Report, “Radial distribution test feeders” IEEE Transactions on Power Systems, August 1991, Vol. 6, No. 3, pp. 975-985.

[26] IEEE Distribution System Analysis Subcommittee Report, “IEEE 4 Node Test Feeder” 2001.

[27] IEEE Distribution System Analysis Subcommittee Report, “IEEE 13 Node Test Feeder” 2004.

[28] IEEE Distribution System Analysis Subcommittee Report, “IEEE 37 Node Test Feeder” 2004.

[29] Teng, J. H. “A Netwrok Topology-based Three-Phase Load Flow for Distribution Systems” Proc. Natl. Sci. Counc. ROC(A), VOl. 24, 2000, pp. 259-264.

[30] Schweppe, F.C., “Power System Static-State Estimation, Part III: Implementation” IEEE Transactions on Power Apparatus and Systems, Vol. PAS-89, No. 1, 1970, pp. 130-135.

[31] Grigsby, Leonard L., Power System Stability and Control, CRC Press, 2007.

[32] Gomez-Exposito, A., Abur, A., de la Villa Jaen, A., Gomez-Quiles, C., “A Multilevel State Estimation Paradigm for Smart Grids,” Proceedings of the IEEE, June 2011, Vol. 99, no: 6, pp. 952-976.

[33] Singh Gyanendra Er., “An algorithm for Observability determination in Bus-System State Estimation using Matlab Simulation” International Journal of Scientific & Engineering Research, October 2013, Vol. 4, Issue 10, pp. 947-955.

APPENDIX A

JACOBIAN MATRIX FOR STATE ESTIMATION OF A THREE PHASE DISTRIBUTION NETWORK

A.1 The elements of Jacobian matrix are expressed as,

The element of Jacobian matrix as shown in () can be expressed as,

$$H=\begin{bmatrix} \frac{\partial P_i}{\partial \theta} & \frac{\partial P_i}{\partial V} \\ \frac{\partial P_{flow}}{\partial \theta} & \frac{\partial P_{flow}}{\partial V} \\ \frac{\partial Q_i}{\partial \theta} & \frac{\partial Q_i}{\partial V} \\ \frac{\partial Q_{flow}}{\partial \theta} & \frac{\partial Q_{flow}}{\partial V} \\ \frac{\partial I}{\partial \theta} & \frac{\partial I}{\partial V} \\ 0 & \frac{\partial V}{\partial V} \end{bmatrix} \quad \text{(A.1)}$$

Real power injection elements:

$$\frac{\partial P_i^p}{\partial \theta_i^p} = \sum_{j=1}^{N} V_i^P V_j^P - (-G_{ij}^P \sin\theta_{ij}^P + B_{ij}^P \cos\theta_{ij}^P) - (V_j^P)^2 B_{ij}^P \quad \text{(A.2)}$$

$$\frac{\partial P_i^P}{\partial \theta_j^p} = V_i^P V_j^P (G_{ij}^P \sin\theta_{ij}^P - B_{ij}^P \cos\theta_{ij}^P) \quad \text{(A.3)}$$

$$\frac{\partial P_i^P}{\partial V_i^p} = \sum_{j=1}^{N} V_j^P \left(G_{ij}^P \cos\theta_{ij}^P + B_{ij}^P \sin\theta_{ij}\right) + V_i G_{ij}^P \quad \text{(A.4)}$$

$$\frac{\partial P_i}{\partial V_j^p} = V_{ij}^P \left(G_{ij}^P \cos\theta_{ij}^P + B_{ij}^P \sin\theta_{ij}^P\right) \quad \text{(A.5)}$$

Real power flow elements:

$$\frac{\partial P_{ij}^P}{\partial \theta_i^p} = V_i^P V_j^P (g_{ij}^P \sin\theta_{ij}^P - B_{ij}^P \cos\theta_{ij}^P) \quad \text{(A.6)}$$

$$\frac{\partial P_{ij}^P}{\partial \theta_j^p} = -V_i^P V_j^P (g_{ij}^P \sin\theta_{ij}^P - b_{ij}^P \cos\theta_{ij}^P) \quad \text{(A.7)}$$

$$\frac{\partial P_{ij}^P}{\partial V_i^p} = -V_j^P \left(g_{ij}^P \cos\theta_{ij}^P + b_{ij}^P \sin\theta_{ij}^P\right) + 2(g_{ij}^P V_i^P) \quad \text{(A.8)}$$

$$\frac{\partial P_{ij}^P}{\partial V_j^p} = -V_i^P (g_{ij}^P \cos\theta_{ij}^P + b_{ij}^P \sin\theta_{ij}^P) \quad \text{(A.9)}$$

Reactive power injection elements:

$$\frac{\partial Q_i^P}{\partial \theta_i^p} = \sum_{j=1}^{N} V_i^P V_j^P (G_{ij}^P \cos\theta_{ij}^P + B_{ij}^P \sin\theta_{ij}^P) - (V_j)^2 G_{ii}^P \quad \text{(A.10)}$$

$$\frac{\partial Q_i^P}{\partial \theta_j^p} = V_i^P V_j^P (-G_{ij}^P \cos\theta_{ij}^P - B_{ij}^P \sin\theta_{ij}^P) \quad \text{(A.11)}$$

$$\frac{\partial Q_i^P}{\partial V_i^P} = \sum_{j=1}^{N} V_j^P \left(G_{ij}^P \sin\theta_{ij}^P - B_{ij}^P \cos\theta_{ij}\right) - V_i^P B_{ii}^P \quad \text{(A.12)}$$

$$\frac{\partial Q_i^P}{\partial V_j^P} = V_i^P (G_{ij}^P \sin\theta_{ij}^P - B_{ij}^P \cos\theta_{ij}^P) \quad \text{(A.13)}$$

Reactive power flow elements:

$$\frac{\partial Q_{ij}^P}{\partial \theta_i^P} = -V_i^P V_j^P (g_{ij}^P \cos\theta_{ij}^P + b_{ij}^P \sin\theta_{ij}^P) \quad \text{(A.14)}$$

$$\frac{\partial Q_{ij}^P}{\partial \theta_j^P} = V_i^P V_j^P (g_{ij}^P \cos\theta_{ij}^P + b_{ij}^P \sin\theta_{ij}^P) \quad \text{(A.15)}$$

$$\frac{\partial Q_{ij}^P}{\partial V_i^P} = -V_i^P \left(g_{ij}^P \sin\theta_{ij}^P - b_{ij}^P \cos\theta_{ij}^P\right) - 2V_{ij}^P b_{ij}^P \quad \text{(A.16)}$$

$$\frac{\partial Q_{ij}^P}{\partial V_j^P} = -V_i^P \left(g_{ij}^P \sin\theta_{ij}^P - b_{ij}^P \cos\theta_{ij}^P\right) \quad \text{(A.17)}$$

Bus voltage elements:

$$\frac{\partial V_i^P}{\partial V_i^P} = 1, \frac{\partial V_i^P}{\partial V_j^P} = 0, \frac{\partial V_i^P}{\partial \theta_i^P} = \frac{\partial V_i^P}{\partial \theta_j^P} = 0 \quad \text{(A.18)}$$

Branch current elements:

$$\frac{\partial I_{ij}^P}{\partial \theta_i^P} = \frac{{g_{ij}^P}^2 + {b_{ij}^P}^2}{I_{ij}^P} V_i^P V_j^P \sin\theta_{ij}^P \quad \text{(A.19)}$$

$$\frac{\partial I_{ij}^P}{\partial \theta_j^P} = -\left(\frac{{g_{ij}^P}^2 + {b_{ij}^P}^2}{I_{ij}^P}\right) V_i^P V_j^P \sin\theta_{ij}^P \quad \text{(A.20)}$$

$$\frac{\partial I_{ij}^P}{\partial V_i^P} = \frac{{g_{ij}^P}^2 + {b_{ij}^P}^2}{I_{ij}^P} (V_i^P - V_j^P \cos\theta_{ij}^P) \quad \text{(A.21)}$$

$$\frac{\partial I_{ij}^P}{\partial V_j^P} = \frac{{g_{ij}^P}^2 + {b_{ij}^P}^2}{I_{ij}^P} (V_j^P - V_i^P \cos\theta_{ij}^P) \quad \text{(A.22)}$$

APPENDIX B

DISTRIBUTION SYSTEM PARAMETERS

B.1 IEEE – 4 bus system

All the data used which are used to perform comprehensive load flow and state estimation for an IEEE 4 node test feeder is given below.

The source is considered to be a substation with a voltage level of 12.47 kV line-to-line.

Table B.1 Data for three phase transformer

Connection type	kVA	kVLL-primary	kVLL-secondary	%R	%X
Step-Down	6,000	12.4	4.1	1	6
Step-Up	6,000	12.4	24.9	1	6

Table B.2 Load data

Bus-4	Phase	Balanced	Unbalanced
Load	A	1800 / 0.9 lag	1275 / 0.85 lag
Load	B	1800 / 0.9 lag	1800 / 0.9 lag
Load	C	1800 / 0.9 lag	2375 / 0.95 lag

The above mentioned loads are connected in closed delta for three wire line configurations and are connected in grounded wye for four wire line configurations.

The phase impedance matrices are given as,

4-wire configuration:

$$Z_{wye}^{abc} = \begin{bmatrix} 0.4576 + 1.078j & 0.1559 + 0.5017j & 0.1535 + 0.3849j \\ 0.1559 + 0.5017j & 0.4666 + 1.0482j & 0.158 + 0.4236j \\ 0.1535 + 0.3849j & 0.158 + 0.4236j & 0.4615 + 1.0651j \end{bmatrix} \Omega/mile$$

3-wire configuration:

$$Z_{delta}^{abc} = \begin{bmatrix} 0.4013 + 1.4133j & 0.0953 + 0.8515j & 0.0953 + 0.7266j \\ 0.0953 + 0.8515j & 0.4013 + 1.4133j & 0.0953 + 0.7802j \\ 0.0953 + 0.7266j & 0.0953 + 0.7802j & 0.4013 + 1.4133j \end{bmatrix} \Omega/mile$$

B.2 IEEE – 13 bus system

All the data which are used to perform comprehensive load flow and state estimation for an IEEE-13 node test system is given below.

Table B.3 Network topology data

Bus A	Bus B	Distance (ft.)	Configuration
1	2	2000	601
2	3	500	603
3	4	300	603
2	5	500	602
5	6	xmer	Z-xmer
2	7	2000	601
7	8	300	604
8	9	300	605
7	10	500	Switch+606
10	11	500	606
7	12	1000	601
8	13	800	607

Table B.4 Data for three phase transformer

	kVA	kV-primary	kV-secondary	%R	%X
Xmer	500	4.1 – G.Wye	0.48 – G.Wye	1.10	2.0

Table B.5 Shunt capacitor data

Bus #	Phase-A	Phase-B	Phase-C
9			100 kVAr
11	200 kVAr	200 kVAr	200 kVAr

Table B.6 Three phase voltage regulator data

Regulator #:	1
Location	Bus 1 – 2
Band-width	2 V
Potential transformer(PT) Ratio	20
Primary current transformer (CT) ratio	700
Phase monitored	A, B and C
Voltage Level	120 V
R and X Settings	3 and 9

Table B.7 Load data for spot loads

Bus #	Load type	Phase-A	Phase-A	Phase-B	Phase-B	Phase-C	Phase-C
		kW	kVAr	kW	kVAr	kW	kVAr
3	Wye-CP	0	0	170.00	125.00	0	0
4	Delta-CZ	0	0	230.00	132.00	0	0
6	Wye-CP	160.00	110.00	120.00	90.00	120.00	90.00
7	Delta-CP	385.00	220.00	385.00	220.00	385.00	220.00
9	Wye-CI	0	0	0	0	170.00	80.00
10	Delta-CI	0	0	0	0	170.00	151.00
11	Wye-CP	485.00	190.00	68.00	60.00	290.00	212.00
13	Wye-CZ	128.00	86.00	0	0 0		0

Table B.8 Load data for distributed loads

Bus A	Bus B	Load type	Phase-A	Phase-A	Phase-B	Phase-B	Phase-C	Phase-C
			kW	kVAr	kW	kVAr	kW	kVAr
2	7	Wye-CP	17.00	10.00	66.00	38.00	117.00	68.00

Impedances:

Configuration 601:

$$Z_{601}^{abc} = \begin{bmatrix} 0.3465 + 1.0179j & 0.1560 + 0.5017j & 0.1580 + 0.4236j \\ 0.1560 + 0.5017j & 0.3375 + 1.0478j & 0.1535 + 0.3849j \\ 0.1580 + 0.4236j & 0.1535 + 0.3849j & 0.3414 + 1.0348j \end{bmatrix} \Omega/mile$$

Configuration 602:

$$Z_{602}^{abc} = \begin{bmatrix} 0.7526 + 1.1814j & 0.1580 + 0.4236j & 0.1560 + 0.5017j \\ 0.1580 + 0.4236j & 0.7475 + 1.1983j & 0.1535 + 0.3849j \\ 0.1560 + 0.5017j & 0.1535 + 0.3849j & 0.7436 + 1.2112j \end{bmatrix} \Omega/mile$$

Configuration 603:

$$Z_{603}^{abc} = \begin{bmatrix} 0.0 + 0.0j & 0.0 + 0.0j & 0.0 + 0.0j \\ 0.0 + 0.0j & 1.3294 + 1.3471j & 0.2066 + 0.4591j \\ 0.0 + 0.0j & 0.2066 + 0.4591j & 1.3238 + 1.3569j \end{bmatrix} \Omega/mile$$

Configuration 604:

$$Z_{604}^{abc} = \begin{bmatrix} 1.3238 + 1.3569j & 0.0 + 0.0j & 0.2066 + 0.4591j \\ 0.0 + 0.0j & 0.0 + 0.0j & 0.0 + 0.0j \\ 0.2066 + 0.4591j & 0.0 + 0.0j & 1.3294 + 1.3471j \end{bmatrix} \Omega/mile$$

Configuration 605:

$$Z_{605}^{abc} = \begin{bmatrix} 0.0 + 0.0j & 0.0 + 0.0j & 0.0 + 0.0j \\ 0.0 + 0.0j & 0.0 + 0.0j & 0.0 + 0.0j \\ 0.0 + 0.0j & 0.0 + 0.0j & 1.3292 + 1.3475j \end{bmatrix} \Omega/mile$$

Configuration 606:

$$Z_{606}^{abc} = \begin{bmatrix} 0.7982 + 0.4463j & 0.3192 + 0.0328j & 0.2849 - 0.0143j \\ 0.3192 + 0.0328j & 0.7891 + 0.4041j & 0.3192 + 0.0328j \\ 0.2849 - 0.0143j & 0.3192 + 0.0328j & 0.7982 + 0.4463j \end{bmatrix} \Omega/mile$$

Configuration 607:

$$Z_{607}^{abc} = \begin{bmatrix} 1.3425 + 0.5124j & 0.0 + 0.0j & 0.0 + 0.0j \\ 0.0 + 0.0j & 0.0 + 0.0j & 0.0 + 0.0j \\ 0.0 + 0.0j & 0.0 + 0.0j & 0.0 + 0.0j \end{bmatrix} \Omega/mile$$

B.3 IEEE – 37 bus system

Table B.9 Data for three phase transformer

	kVA	kV-primary	kV-secondary	%R	%X
Xmer	500	4.8 – Delta	0.48 – Delta	0.090	1.810

Table B.10 Load data for spot loads

Node	Bus #	Load type	Phase-A	Phase-A	Phase-B	Phase-B	Phase-C
		kW	kVAr	kW	kVAr	kW	kVAr
2	Delta-CP	140.00	70.00	140.00	70.00	350.00	175.00
5	Delta-CP	0	0	0	0	85.00	40.00
6	Delta-CP	8.00	4.00	85.00	40.00	0	0
7	Delta-CP	0	0	0	0	85.00	40.00
9	Delta-CI	17.00	8.00	21.00	10.00	0	0
10	Delta-CZ	85.00	40.00	0	0	0	0
11	Delta-CP	0	0	0	0	85.00	40.00
13	Delta-CZ	0	0	42.00	21.00	0	0
14	Delta-CI	0	0	140.00	70.00	21.00	10.00
16	Delta-CP	0	0	42.00	21.00	0	0
18	Delta-CP	0	0	0	0	42.00	21.00
19	Delta-CI	42.00	21.00	0	0	0	0
20	Delta-CP	42.00	21.00	42.00	21.00	42.00	21.00
22	Delta-CZ	0	0	0	0	85.00	40.00
25	Delta-CZ	0	0	85.00	40.00	0	0
27	Delta-CI	0	0	0	0	42.00	21.00
28	Delta-CP	85.00	40.00	0	0	0	0
29	Delta-CP	0	0	0	0	42.00	21.00
31	Delta-CI	0	0	42.00	21.00	0	0
32	Delta-CP	0	0	0	0	85.00	40.00
33	Delta-CZ	140.00	70.00	0	0	0	0
34	Delta-CP	126.00	62.00	0	0	0	0
37	Delta-CP	0	0	0	0	42.00	21.00

Table B.11 Network topology data

Bus A	Bus B	Distance (ft.)	Configuration
1	2	5280	722
2	3	960	722
3	4	400	724
4	5	240	724
4	6	320	724
3	7	360	723
7	8	520	723
8	9	80	724
9	10	520	724
8	11	800	723
11	12	920	724
12	13	760	724
12	14	120	724
11	15	600	723
15	16	280	724
3	17	1320	722
17	18	240	724
18	19	280	723
19	20	200	724
19	21	280	724
17	22	600	723
22	23	200	723
23	24	xmer	Z-xmer
23	25	600	723
23	26	320	723
26	27	320	723
26	28	320	723
28	29	560	723
29	30	520	724
30	31	1280	724
30	32	200	724
29	33	640	723
33	34	400	723
34	35	400	723
35	36	200	724
35	37	400	723

Impedances:

Configuration 721:

$$Z_{721}^{abc} = \begin{bmatrix} 0.2926 + 0.1973j & 0.0673 - 0.0368j & 0.0337 - 0.0417j \\ 0.0673 - 0.0368j & 0.2646 + 0.1900j & 0.0673 - 0.0368j \\ 0.0337 - 0.0417j & 0.0673 - 0.0368j & 0.2926 + 0.1973j \end{bmatrix} \Omega/mile$$

Configuration 722:

$$Z_{722}^{abc} = \begin{bmatrix} 0.4751 + 0.2973j & 0.1629 - 0.0326j & 0.1234 - 0.0607j \\ 0.1629 - 0.0326j & 0.4488 + 0.2678j & 0.1629 - 0.0326j \\ 0.1234 - 0.0607j & 0.1629 - 0.0326j & 0.4751 + 0.2973j \end{bmatrix} \Omega/mile$$

Configuration 723:

$$Z_{723}^{abc} = \begin{bmatrix} 1.2936 + 0.6713j & 0.4871 + 0.2111j & 0.4585 + 0.1521j \\ 0.4871 + 0.2111j & 1.3022 + 0.6326j & 0.4871 + 0.2111j \\ 0.4585 + 0.1521j & 0.4871 + 0.2111j & 1.2936 + 0.6713j \end{bmatrix} \Omega/mile$$

Configuration 724:

$$Z_{724}^{abc} = \begin{bmatrix} 2.0952 + 0.7758j & 0.5204 + 0.2738j & 0.4926 + 0.2123j \\ 0.5204 + 0.2738j & 2.1068 + 0.7398j & 0.5204 + 0.2738j \\ 0.4926 + 0.2123j & 0.5204 + 0.2738j & 2.0952 + 0.7758j \end{bmatrix} \Omega/mile$$

Table B.12 Three phase voltage regulator data

Regulator #:	1
Location	Bus 1 – 2
Band-width	2 V
Potential transformer (PT) Ratio	40
Primary current transformer (CT) ratio	350
Phase monitored	A-B-C
Voltage Level	120 V
R and X Settings	1.5 and 3